TU Delft

Delft University of Technology

Photochemical fate of quaternary ammonium compounds (QACs) and degradation pathways predication through computational analysis

Mohapatra, Sanjeeb; Li Xian, Jovina Lew; Gálvez-Rodríguez, Andy; Ekande, Onkar Sudhir; Drewes, Jörg E.; Gin, Karina Yew-Hoong

DOI
10.1016/j.jhazmat.2024.133483

Publication date
2024

Document Version
Final published version

Published in
Journal of Hazardous Materials

Citation (APA)
Mohapatra, S., Li Xian, J. L., Gálvez-Rodríguez, A., Ekande, O. S., Drewes, J. E., & Gin, K. Y.-H. (2024). Photochemical fate of quaternary ammonium compounds (QACs) and degradation pathways predication through computational analysis. *Journal of Hazardous Materials*, *465*, Article 133483. https://doi.org/10.1016/j.jhazmat.2024.133483

Important note
To cite this publication, please use the final published version (if applicable).
Please check the document version above.

Copyright
Other than for strictly personal use, it is not permitted to download, forward or distribute the text or part of it, without the consent of the author(s) and/or copyright holder(s), unless the work is under an open content license such as Creative Commons.

Takedown policy
Please contact us and provide details if you believe this document breaches copyrights.
We will remove access to the work immediately and investigate your claim.

This work is downloaded from Delft University of Technology.
For technical reasons the number of authors shown on this cover page is limited to a maximum of 10.

Journal of Hazardous Materials 465 (2024) 133483

Contents lists available at ScienceDirect

Journal of Hazardous Materials

journal homepage: www.elsevier.com/locate/jhazmat

Review

Photochemical fate of quaternary ammonium compounds (QACs) and degradation pathways predication through computational analysis

Sanjeeb Mohapatra [a,b,c], Jovina Lew Li Xian [a], Andy Galvez-Rodriguez [d], Onkar Sudhir Ekande [e], Jörg E. Drewes [f], Karina Yew-Hoong Gin [a,b,g,*]

[a] NUS Environmental Research Institute, National University of Singapore, T-Lab Building, 5A Engineering Drive 1, 117411, Singapore
[b] Energy and Environmental Sustainability for Megacities (E2S2) Phase II, Campus for Research Excellence and Technological Enterprise (CREATE), 1 CREATE Way, 138602, Singapore
[c] Department of Water Management, Faculty of Civil Engineering and Geosciences, Delft University of Technology, P.O Box 5048, 2600 GA Delft, the Netherlands
[d] Department of Chemistry, University of Alberta, Edmonton, Canada
[e] Environmental Engineering Division, Department of Civil Engineering, Indian Institute of Technology Madras, Chennai 600036, Tamil Nadu, India
[f] Chair of Urban Water Systems Engineering, Technical University of Munich, 85748 Garching, Germany
[g] Department of Civil & Environmental Engineering, National University of Singapore, Engineering Drive 2, 117576, Singapore

HIGHLIGHTS

- QACs are resistant to direct photodegradation due to their stable structure.
- Photocatalytic degradation of QACs using TiO_2 catalyst has been found effective.
- Computational approaches have revealed degradation pathways for QACs.
- QACs' degradation products may be more toxic than the parent QACs.

GRAPHICAL ABSTRACT

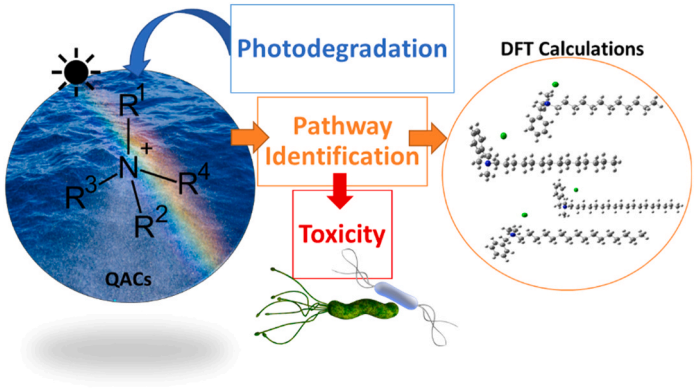

ARTICLE INFO

Editor: Jelena Radjenovic

Keywords:
Quaternary ammonium compounds (QACs)
Photochemical fate
Computational analysis
Degradation pathway

ABSTRACT

Quaternary ammonium compounds (QACs) are commonly used in many products, such as disinfectants, detergents and personal care products. However, their widespread use has led to their ubiquitous presence in the environment, posing a potential risk to human and environmental health. Several methods, including direct and indirect photodegradation, have been explored to remove QACs such as benzylalkyldimethyl ammonium compounds (BACs) and alkyltrimethyl ammonium compounds (ATMACs) from the environment. Hence, in this research, a systematic review of the literature was conducted using PRISMA (Preferred Reporting Items for Systematic Reviews and Meta-Analysis) method to understand the fate of these QACs during direct and indirect photodegradation in UV/H_2O_2, UV/PS, UV/PS/Cu^{2+}, UV/chlorine, VUV/UV/chlorine, O_3/UV and UV/O_3/TiO_2 systems which produce highly reactive radicals that rapidly react with the QACs, leading to their degradation. As

* Corresponding author at: NUS Environmental Research Institute, National University of Singapore, T-Lab Building, 5A Engineering Drive 1, 117411, Singapore.
E-mail address: ceeginyh@nus.edu.sg (K.Y.-H. Gin).

https://doi.org/10.1016/j.jhazmat.2024.133483
Received 24 July 2023; Received in revised form 30 November 2023; Accepted 8 January 2024
Available online 11 January 2024
0304-3894/© 2024 The Author(s). Published by Elsevier B.V. This is an open access article under the CC BY-NC license (http://creativecommons.org/licenses/by-nc/4.0/).

a result of photodegradation, several transformation products (TPs) of QACs are formed, which can pose a greater risk to the environment and human health than the parent QACs. Only limited research in this area has been conducted with fewer QACs. Hence, quantum mechanical calculations such as density functional theory (DFT)-based computational calculations using Gaussian09 software package were used here to explain better the photo-resistant nature of a specific type of QACs, such as BACs C12–18 and ATMACs C12, C14, C18, and their transformation pathways, providing insights into active sites participating in the phototransformation. Recognizing that different advanced oxidation processes (AOPs) come with pros and cons in the elimination of QACs, this review also highlighted the importance of implementing each AOP concerning the formation of toxic transformation products and electrical energy per order (EEO), especially when QACs coexist with other emerging contaminants (ECs).

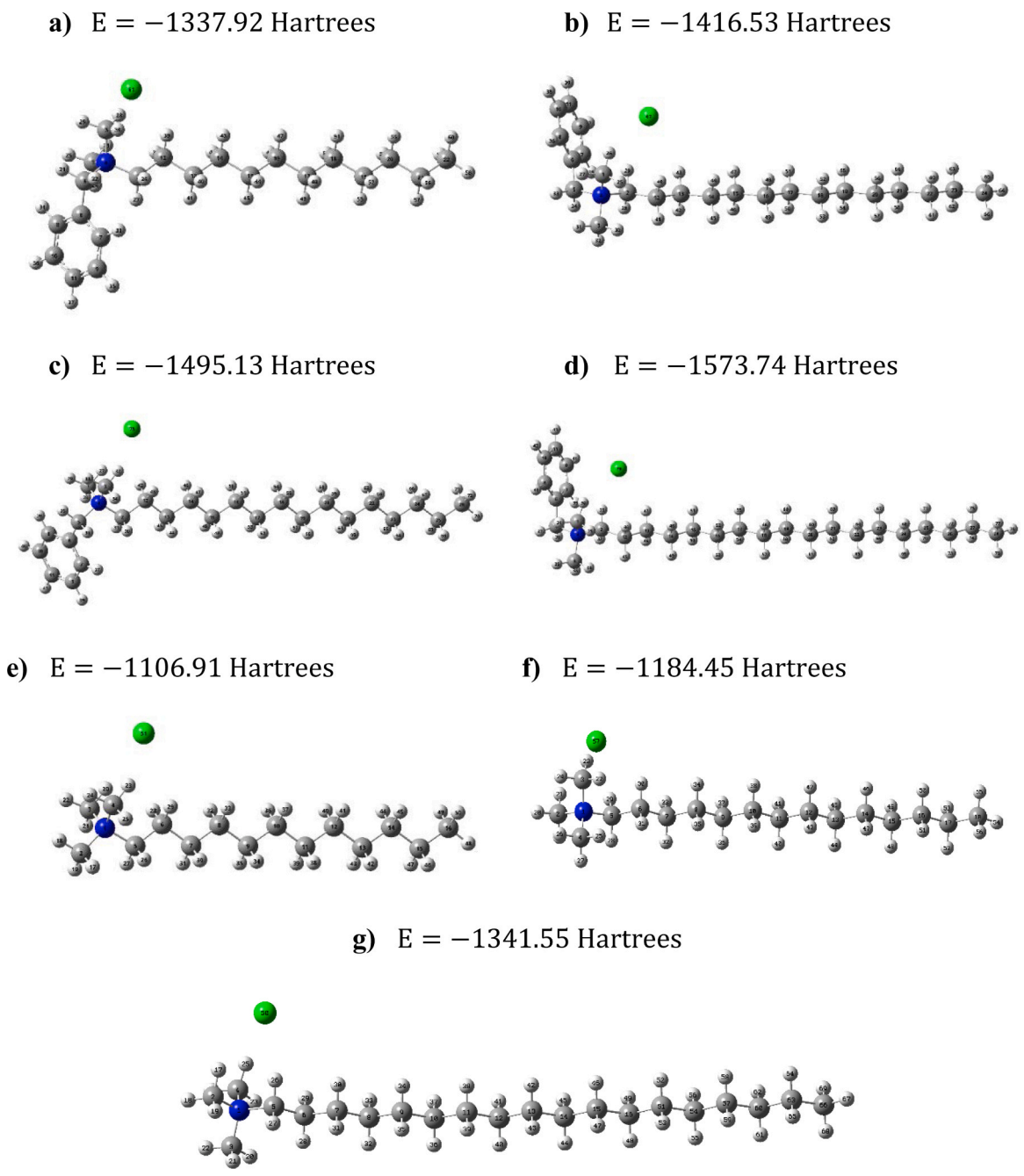

Fig. 1. Structure and electronic energy (E) without zero point energy correction for selected QACs at M06–2X/6–311 G(d,p) level of theory: a) BAC C12, b) BAC C14, c) BAC C16, d) BAC C18, e) ATMAC C12, f) ATMAC C14 and g) ATMAC C18. Hydrogen, carbon, nitrogen, and chlorine atoms are represented by white, gray, blue, and green spheres, respectively.

1. Introduction

Quaternary ammonium compounds (QACs) are cationic surfactants with bactericidal and virucidal properties. Thus, these compounds have been used as active ingredients in commonly found disinfectants and cleaning agents in hospitals, restaurants, and homes [7–9,43–45]. Compared to QACs used in personal care products, which can have alkyl chains as long as 22, QACs used in cleaning and disinfection goods typically have lower alkyl chain lengths (C8–C16) [3]. They have also gotten much attention due to their application in the synthesis of nanocomposites [56], as a source of bromide during photocatalysis experiments [17], and even in the design of pH-Swing membrane for contaminant removal [64]. The general structure of a QAC consists of a positively charged nitrogen atom attached to at least one hydrophobic hydrocarbon chain, i.e., alkyl groups (Fig. 1). Most QACs also have halogen anions attached to them, which determines the amphiphilic nature of the compound [49]. As such, QACs are positively charged at neutral pH ranges and are more easily adsorbed onto negatively charged surfaces such as sludge, soil, and sediments [5]. For QACs, there are several different and complicated nomenclatures. Benzylalkyldimethyl ammonium compounds (BACs), alkyltrimethyl ammonium compounds (ATMACs), and dialkyldimethyl ammonium compounds (DADMACs) are examples of QACs that are often mentioned in environmental research [3].

Routes of exposure of QACs to humans include inhalation, dermal contact, and oral ingestion. Studies have shown that exposure to high concentrations of QACs through inhalation or ingestion can result in cell death by disrupting mitochondria functions, adversely affecting ATP production [14,52]. There have also been a rising number of observations of asthma occurrences among healthcare workers exposed to disinfectants with QACs [18,20,45]. Furthermore, other studies reported QACs in the bloodstream, with a finding of 80% present in 43 human volunteers [24]. QACs leading to more widespread antimicrobial resistance in bacteria is another crucial issue that needs to be considered [39]. Studies have shown that both Gram-negative and Gram-positive bacteria display cross-resistance traits. For instance, Gram-negative *Escherichia coli's* minimum inhibitory concentration (MIC) to QACs and antibiotics increased by 2 to 7 folds and 1 to 116 folds, respectively [49] and Gram-positive methicillin-resistant *Staphylococcus aureus's* (MRSA) MIC to β-lactam antibiotics increased by 1 to 16 folds [1]. Research has reported on the reduced susceptibility of Salmonella enterica to the disinfection process with QACs [6]. Another study found that benzyldimethyltetradecyl ammonium chloride (BAC C14) interferes with the physiological and metabolic processes in Microcystis cells and induces the formation and release of microcystin, which could potentially harm aquatic ecosystems [29].

QACs have been detected in wastewater, sludge, surface water, sediments, soil, and sewage-impacted areas [21,22,36–38]. Most QACs end up in wastewater treatment plants (WWTPs) via sewage systems, and residual concentrations can be released into the aqueous environment via effluent of conventional biological nutrient removal plants [12,55]. The concentration of QACs found in surface water and treated wastewater worldwide varies from less than 1 μg/L to about 100 μg/L. In untreated wastewater, their concentration can be up to twelve times higher, reaching around 1200 μg/L [49,50].

The rapid use of QACs during the pandemic has raised additional concern due to their possible elevated level in the affected environmental matrices and poor removal during biodegradation at WWTPs [50]. The environmental fate and toxicity of QACs are influenced by the type of bonded substituents and the alkyl chain length [3]. A recent study suggests that QACs can significantly inhibit microbial activity at the WWTP [62], similar to the effects observed for BACs. For instance, benzalkonium chloride (BAC C12 or DDBAC) shock treatment can cause the destruction of aerobic granular sludge structure by reducing its particle size, ultimately resulting in particle disintegration [62]. By combining the effects of cell lysis, electric neutralization, and improved hydrophobicity, the presence of QACs has been shown to promote sludge solubilization but inhibit methanogenesis due to the buildup of volatile fatty acids and the susceptibility of methanogens to QACs [66].

So far, only a few attempts have been made using advanced oxidation-based treatment technologies to remove these compounds from environmental matrices and water streams [21,35,36]. However, it is important to note that while the parent compound may be degraded, the formation of transformation products (TPs) during degradation with a similar or elevated level of toxicity can still pose a risk, as reported for dodecyltrimethylammonium chloride (DTAC or ATMAC C12) [36]. Except for BAC C12 and ATMAC C12, studies highlighting the photo-trasnforamtion of other QACs of longer carbon chain lengths are still rare in the literature. Therefore, further research is needed to better understand the potential photochemical fate of these QACs and probable transformation pathways leading to toxic product formation. Recently, powerful software packages such as Gaussian09 have been used in the scientific domain to study the degradation pathway of ECs, such as pharmaceuticals, as they allow for the exploration of various reaction pathways and the prediction of potential degradation products [51]. The underlying models of these packages are based on the principles of quantum mechanics and provide accurate and reliable calculations of molecular structures, energies, and properties. With its user-friendly interface and extensive range of computational tools, such software is widely regarded as a valuable tool for researchers in the field of environmental engineering. Such a tool can also be used to study the photodegradation pathways for QACs.

Thus, this bibliometric study aims to collate the available information on the photochemical fate of QACs and explore the extent of their degradation through direct, indirect, and advanced oxidation processes (AOPs). The cost of various techniques applied in the AOPs for QACs is discussed, including a comprehensive comparison of these degradation methods. The discussion encompasses the advantages, disadvantages, and potential improvements associated with each technique including electrical energy per order (EEO). Furthermore, this research explains the possible formation of TPs and photo transformation degradation pathways through computational analysis for the most used QACs such as BACs and ATMACs. The major focus of this work is a step-by-step approach to conducting computational analysis on the aforementioned QACs.

2. Methodology

2.1. Review of literature

This bibliometric study utilized the PRISMA (Preferred Reporting Items for Systematic Reviews and Meta-Analysis) method, which involves four distinct levels: Identifying, Screening, Eligibility, and Inclusion criteria. These levels were carried out in three stages. In the first stage, a suitable search engine such as Google Scholar was fed with keywords as Google Scholar provides a diverse range of journal availability and more recently published works. The keywords used in the search engine are the photochemical fate of QACs, photodegradation of QACs, ATMAC C12–18, DADMAC C8–18 and BAC C12–18. Around 200 documented results were initially obtained, and the literature was screened based on several inclusive criteria. The screening process involved selecting only peer-reviewed journal articles. The articles were also categorized into different sub-areas based on the subject areas that fell under the immediate scope of the study, such as direct photodegradation, indirect photodegradation, and degradation pathways for QACs, including experiments conducted using both synthetic and environmental samples under different irradiance condition (Table 1). Finally, any duplicates in the published articles were removed to ensure no overlap in the final dataset. Finally, 16 articles were used to explain the direct, indirect, and, most importantly, photodegradation pathways of QACs. The dataset of degradation products and pathways published articles were then selected for computational analyses.

Table 1
Irradiance source and lamps used for QAC degradation in the literature.

Lamp details	Irradiance condition	References
Xenon (Xe) lamp	**a)** Open quartz cell using an Xe lamp (IFP 1200) with a flash energy of 100 J, Alpha-02 pulse UV-radiation apparatus with an average electric power on the lamp of 200 W, 100μs, f = 2 Hz	[53]
	b) Solar simulator (SUNTEST CPS$^+$, ATLAS, Chicago, USA) equipped with a Xe lamp (1500 W) emitting radiation similar to sunlight in the range of 300-800 nm	[46]
	c) 1500 W xenon arc lamp and 290 nm cutoff filter used in an Atlas Suntest CPS+ solar simulator	[21]
Mercury (Hg) lamp	**a)** 75 W, λ < 330 nm, under magnetic agitation, in a 72 ml Pyrex vessel	[57]
	b) 30-W low-pressure, in a merry-go-round apparatus, 254 nm (EIKOHSHA, EL-J-60)	[28]
	c) Quasi-collimated beam apparatus equipped with two 87 W low pressure Hg lamps (254 nm, Light Sources Inc., USA)	[25]
	d) Quasi-collimated beam (41 W low-pressure Hg lamps 254 nm, Light Sources Inc., USA)	[36]
	e) Low-pressure Hg lamp with a quasi-collimated beam (Light sources, Orange, CT, USA)	[34]
	f) Medium pressure mercury UV lamp (Heraeus, Hanau, Germany) 150 W ($UV_{190} < \lambda < VIS_{600}$)	[33]
	g) Quasi-collimated beam with wavelength of 254 nm, produced by two 41 W low-pressure Hg lamps (Light Sources, Orange, CT, USA)	[35]
	h) 9 W low-pressure mercury lamp (Philips TUV PL-L) with a maximum emission wavelength of 254 nm	[67]
UV/VUV lamp	**a)** Black light tubular UV lamp (Philips TLD/08, 15 W, 350 nm < λ < 410 nm, maximum emission at 366 nm)	[40]
	b) 48 W lamp (GZW48D15Y-Z436, Comwin, Guangdong, China) device needs to be filled with nitrogen before startupto prevent reaction between VUV and air.	[65]
LED light	**a)** 0.130 W/m^2, filtered through a polycarbonate case that removed UV light	[30]

2.2. Computational analysis

Quantum mechanical calculations were performed to explain and provide insights into the transformation pathways of the selected QACs, such as benzylalkyldimethylethylammonium compounds (BACs) and alkyltrimethyl ammonium compounds (ATMACs) for which TPs are reported in the literature. First, the structure for the selected QACs under study was drawn using HyperChem 7.01 [27] and subsequently pre-optimized using PM3 semiempirical Hamiltonian [58] (Fig. 1). Further semiempirical calculations were carried out in MOPAC2016 (Molecular Orbital Package) Stewart [59] using the robust PM7 Hamiltonian [23]. Density Functional Theory (DFT) was used as the final optimization step for the QACs, specifically the exchange-correlation functional M06–2X [10] and the 6–311 G(d,p) basis function. This conjunction has been successfully applied in previous computational studies [16,2,26]. All DFT optimisation calculations were performed in the Gaussian09 software package [13]. Solvent effects were considered using the continuum solvation model based on solute electron density and solvent dielectric constant, SMD (water as solvent). The previously mentioned theory level was used to obtain and characterize the Frontier Molecular Orbitals (FMO) of the QACs (Fig. 2). Further, unrestricted single-point DFT calculations were carried out to determine the most active sites of the molecules toward nucleophilic and electrophilic attacks at UM06–2X/6–311 G(2df,2pd). First, output files were used to calculate the charge distribution of the QACs (neutral, anionic and cationic species) by applying the Atomic Dipole Corrected Hirshfeld (ADCH) population analysis [42] in the Multiwfn software [41]. This model fixes some drawbacks of the previous Hirshfeld model, in which charges are too small and poor reproducibility of molecular dipole moments. As determined during the literature review on the photodegradation pathways of selected QACs, the conjunction between electrophilic, nucleophilic and radical reactions plays a critical role in the production of the degradation products. Thus, the charge distribution was employed to calculate the nucleophilic, electrophilic and radical condensed functions [4,15] as follows (Fig. 3):

$$f_A^+ = q_A^N - q_A^{N+1} \quad \text{(nucleophilic Fukui function)} \tag{1}$$

$$f_A^- = q_A^{N-1} - q_A^N \quad \text{(electrophilic Fukui function)} \tag{2}$$

$$f_A^0 = \frac{q_A^{N-1} - q_A^{N+1}}{2} \quad \text{(radical Fukui } \textit{function}\text{)} \tag{3}$$

where q_A^N, $q_A^{N+1}$and q_A^{N-1} stand for the charge of atom A when the total number of electrons is N (neutral species), N +1 (anionic species) and N −1 (cationic species), respectively. The conjunction between frontier molecular orbital characterization and condensed Fukui function helped to study the QACs' degradation pathways. A similar methodology has been previously used to predict the degradation pathways of pharmaceuticals in an aqueous solution [51].

3. Direct and indirect photodegradation

Direct photolysis is considered one of the natural attenuation mechanisms for emerging contaminants (ECs) in natural water [47,48]. However, only limited attempts were made to study QACs' direct photolysis in the lab or natural environment. A study by Itoh et al. [28] evaluated the extent of photodegradation for two benzyl-containing ammonium salts such as p-alkylbenzyltrimethylammonium halides and alkylbenzyldimethylammonium halides. Significant degradation of 93–100% was observed during ultraviolet (UV) irradiance for 5 h due to the heterolytic and homolytic cleavages of the benzyl-nitrogen bond (Table S1). Following this study, after five years, Hora & Arnold [21] evaluated the extent of photodegradation for benzyldimethyl-n-dodecylammonium chloride (BAC C12), benzyldimethyltetradecyl-ammonium chloride hydrate (BAC C14) and benzethonium chloride (BZT) in Mississippi river water under a solar simulator and natural sunlight (Table S2). No significant degradation was observed for BAC C12 and C14 under the solar simulator and outdoor river water. The bimolecular rate constants under solar simulator were $K_{OH,\ BAC\ C12} = 1.1 \times 10^{10}\ M^{-1}\ s^{-1}$ and $K_{OH,\ BAC\ C14} = 1.2 \times 10^{10}\ M^{-1}\ s^{-1}$, and under natural light, they were $K_{OH,\ BAC\ C12} = 1.2 \times 10^{10}\ M^{-1}\ s^{-1}$ and $K_{OH,\ BAC\ C14} = 1.2 \times 10^{10}\ M^{-1}\ s^{-1}$. Whereas BZT showed significant degradation under solar simulator with a rate constant ($K_{OH,\ BZT}$) of $9.3 \times 10^9\ M^{-1}\ s^{-1}$. In 2023, Joshi et al. [30] evaluated the extent of photodegradation for 4,4-difluoro-4-bora-3a,4a-diaza-s-indacene (BODIPY 17). The compound was found to be unstable and undergoes degradation in the dark and light easily by 77% and 35%, respectively. However, it took around 10 h for the compound to degrade in the dark and only 10 min during light exposure. Except for BODIPY 17, which is commonly used as photosensitizers, most of the studied QACs are resistant to direct photolysis, possibly attributed to their stable structure. Hence, several attempts were made to study their fate during indirect photodegradation and photocatalytic degradation, as described in the following sections.

3.1. Role of natural organic matter

Depending on the experimental conditions and nature of QACs, dissolved or natural organic matter (DOM/NOM) either enhances or decreases the rates of QAC degradation. Due to their hydrophobic nature, QACs are normally sorbed onto DOM, which is ubiquitous in natural waters and behaves as a sink for QACs [21]. NOM can disrupt QAC removal through radical scavenging and UV light scattering [34]. It reacts with radicals such as ·OH and $SO_4{\cdot}^-$, hence leading to radical scavenging [35]. However, Miłosek et al. [46] also found that NOM can act as a photosensitizer, allowing for a series of radical reactions

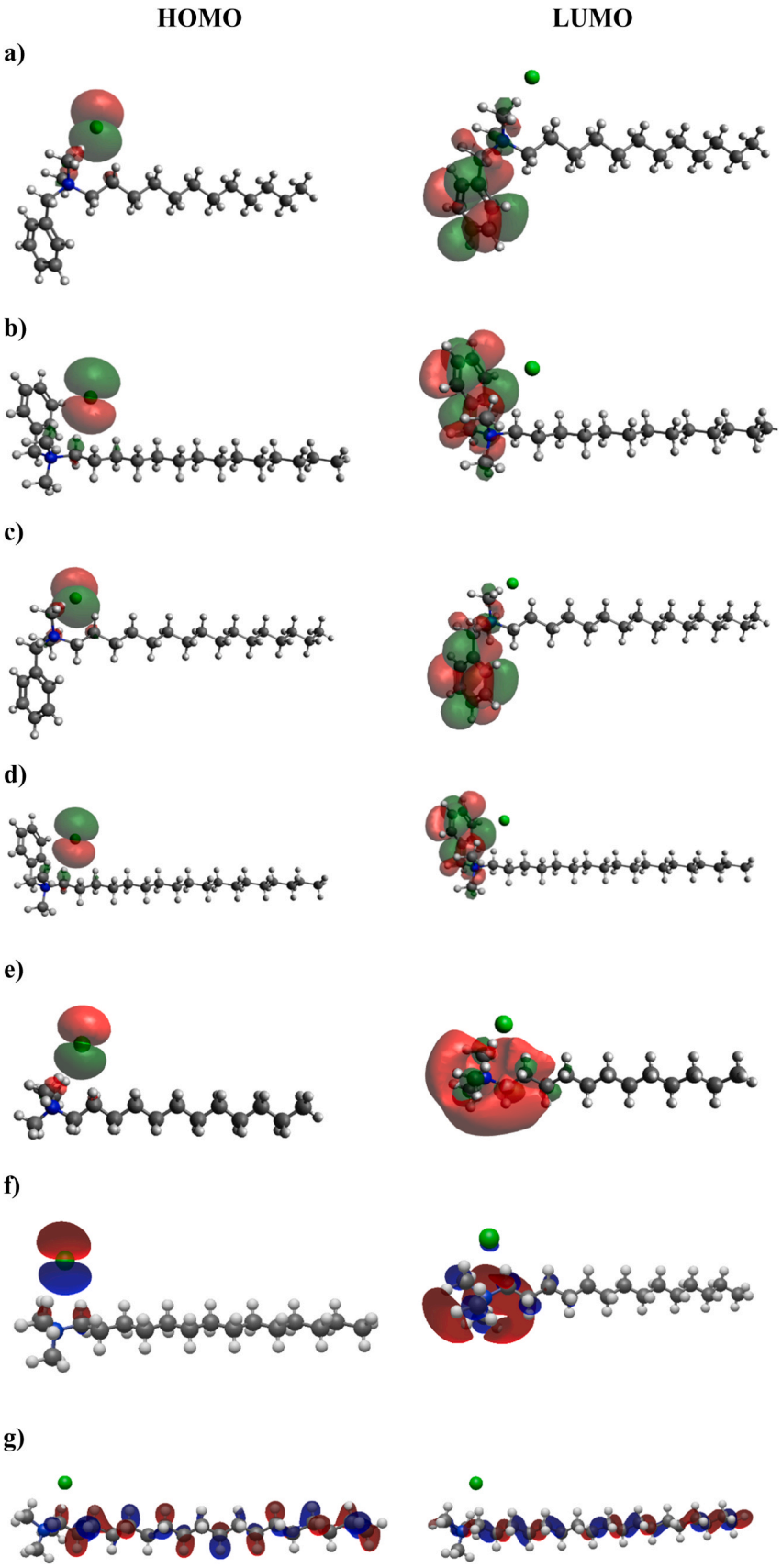

Fig. 2. Frontier molecular orbitals of selected QACs at M06–2X/6–311 G(d,p) level of theory: a) BAC12, b) BAC14, c) BAC16, d) BAC18, e) ATMAC C12, f) ATMAC C14 and g) ATMAC C18. HOMO orbitals are shown on the left side while LUMO orbitals are on tare the right side. Hydrogen, carbon, nitrogen, and chlorine atoms are represented by white, gray, blue, and green spheres respectively.

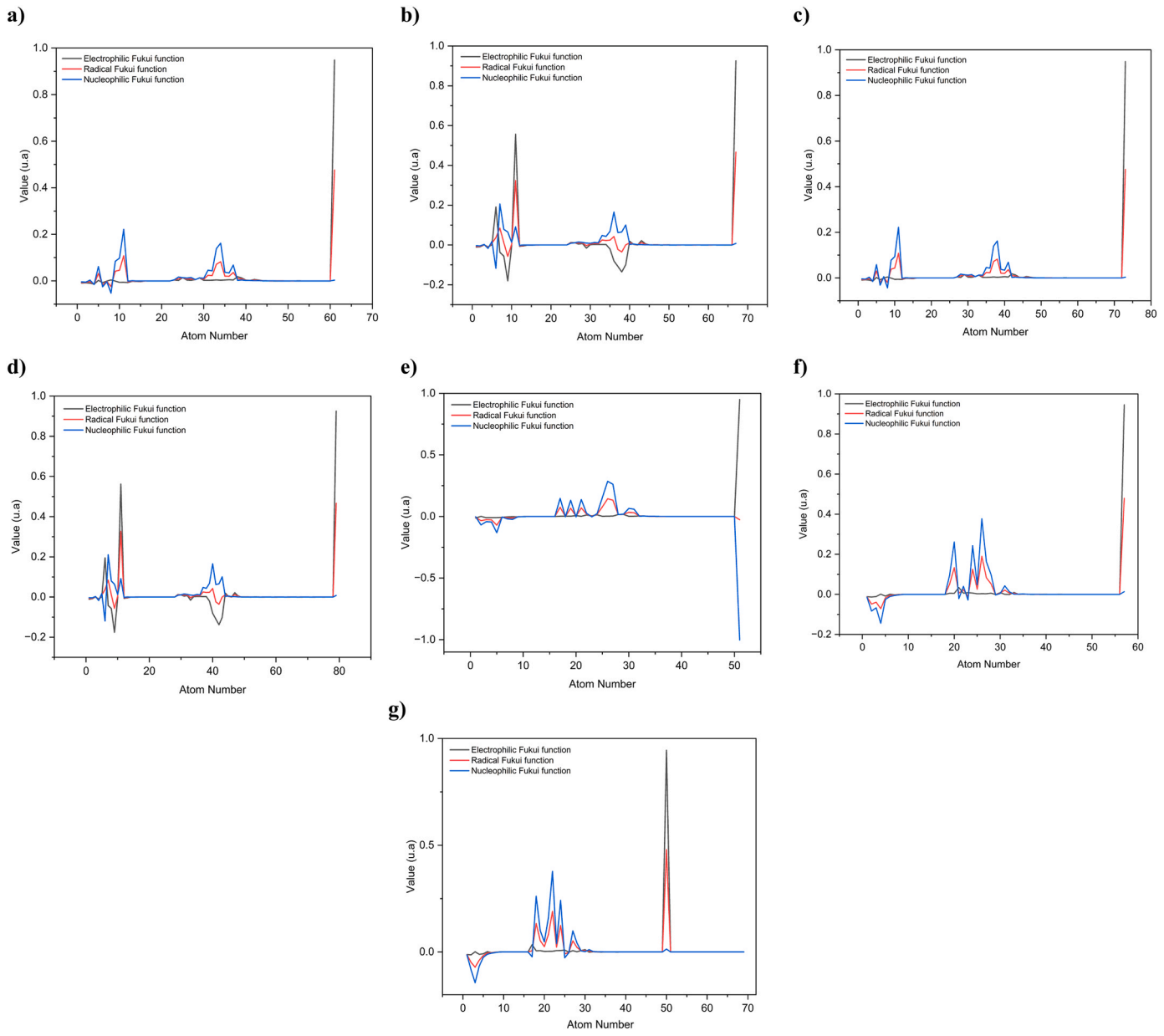

Fig. 3. Representation of electrophilic, nucleophilic and radical Fukui functions of a) BAC C12, b) BAC C14, c) BAC C16, d) BAC C18, e) ATMAC C12, f) ATMAC C14 and g) ATMAC C18 at UM06–2X/6–311(2df,2pd) level of theory (Table S14-S20). Electrophilic, radical, and nucleophilic Fuki functions are represented by black, red, and blue lines, respectively.

resulting in quicker degradation of tetraoctylammonium bromide (TOAB).

3.2. Role of cations and anions

A study by Lee et al. [34] on the UV/PS/Cu^{2+} system found that the cations Fe^{2+}, Mn^{2+}, Zn^{2+} and Mg^{2+} in reverse osmosis concentrates could increase the degradation of dodecyltrimethylammonium chloride (DTAC or ATMAC C12) and dodecyl dimethyl benzyl ammonium chloride (DDBAC or BAC C12). These cations aided in the formation of sufficient $SO_4^{\cdot-}$, which further contributed to the increased degradation of QACs. Anions such as HCO_3^-/CO_3^{2-} can have an inhibitory effect on the degradation of QACs as they can react with the oxidative radicals [25] resulting in less reactive $CO_3^{\cdot-}$. Meanwhile, anions like Cl^- can have dual effects. A study by Lee et al. [35] showed that Cl^- can react with $SO_4^{\cdot-}$ to form reactive chlorine species and thus, convert $SO_4^{\cdot-}$ to ·OH, enhancing the degradation of QACs. However, at higher concentrations, Cl^- has an inhibitory effect on the degradation process. NO_3^- can also be transformed into reactive nitrogen species with low redox potentials, which then reacts with ·OH, decreasing the degradation of QACs.

3.3. Photodegradation of QACs in H_2O_2, UV/PS, UV/Cl, UV/O_3 and UV/PS/Cu^{2+} systems

For the first time, Panich et al. [53] evaluated the extent of indirect photodegradation of dodecyl trimethylammonium bromide (DTAB) by hydrogen peroxide (H_2O_2). Although no degradation was observed under dark conditions, DTAB degradation significantly increased under light conditions as the concentration of H_2O_2 increased (Table S3). When the concentration of H_2O_2 increased from 0 mg/L to 25 mg/L, degradation increased from 11% in 20 min to 80% in 10 min. When the concentration of H_2O_2 was increased to 50–100 mg/L, complete degradation of DTAB was achieved in 15 min. While the synergistic effects of UV and H_2O_2 play a critical role at a low concentration of H_2O_2,

at high concentration, the effect of direct oxidation by H_2O_2 and UV fluence cannot be ruled out.

Similarly, Lee et al. [36] evaluated the extent of indirect photodegradation of another type of QAC, i.e., ATMAC C12 in UV/PS (persulfate) AOP (Table S4), which produced powerful radicals such as ·OH and SO_4·$^-$ with high redox potentials of 1.8–2.7 V and 2.5–3.1 V, respectively. Degradation of ATMAC C12 hardly occurred under UV direct photolysis or PS oxidation but was significantly enhanced to 91% when UV and PS were combined. This is because of the synergistic effect of UV and PS that can rapidly react with ATMAC C12. In another study conducted on BAC C12 in the UV/PS system [35], it was found that BAC C12 degradation after 15 min was higher in UV/PS systems at 83% compared to PS-only and UV-only systems at 19% and 41%, respectively. This was due to the synergistic effect of UV/PS (Table S5). The degradation of BAC C12 also increased from 50% to 90% as the concentration of PS increased, highlighting a positive correlation between the number of radicals generated and the dosage of PS.

These two studies were later expanded by Lee et al. [34] to evaluate the extent of indirect photodegradation for ATMAC C12 and BAC C12 in deionized (DI) water in an UV/PS/Cu^{2+} systems (Table S6). Under UV only, PS only and Cu^{2+} only conditions, degradation of ATMAC C12 and BAC C12 barely occurred within 4 min. Under PS/Cu^{2+} conditions, slight degradation of ATMAC C12 and BAC C12 of 5% and 4%, respectively, were observed, as Cu^{2+} has low reactivity towards PS for generating SO_4·$^-$. Under UV/PS/Cu^{2+} and UV/PS conditions for 4 min, significant degradation of ATMAC C12 of 96.2% and 65%, respectively, and BAC C12 of 98.5% and 66%, respectively, was observed. Two possible reasons could explain such an efficient removal. Firstly, Cu^{2+} may directly react with PS to produce $SO_4^{\cdot-}$. Secondly, Cu^{2+} may contribute in generating more $SO_4^{\cdot-}$ or other radical species. However, SO_4·$^-$ generation is typically affected by the pH of the solution. In general, an increase in pH reduces the SO_4·$^-$ generation. However, with the increased generation of ·OH at a high pH of 11, $SO_4^{\cdot-}$ oxidized OH^- to form ·OH radicals. Thus, high concentrations of ·OH further increased the removal of ATMAC C12 and BAC C12 26 and 8 times, respectively.

$$2S_2O_8^{2-} + 2\,H_2O \rightarrow 3SO_4^{2-} + SO_4^{\cdot-} + O_2^{\cdot-} + 4\,H^+ \quad (4)$$

$$SO_4^{\cdot-} + OH^- \rightarrow {}^{\cdot}OH + SO_4^{2-} \quad (5)$$

$$HOCl \rightarrow Cl^{\cdot} + {}^{\cdot}OH \quad (6)$$

$$HOCl \leftrightarrow OCl^- + H^+ \ (pK_a = 7{\cdot}6) \quad (7)$$

There were three more studies on three different systems, i.e., UV/chlorine [25], vacuum ultraviolet (VUV)/UV/chlorine [65], and O_3/UV [67] systems, where BAC C12 removals were reported. The study by Huang et al. [25] reported 65% removal for BAC C12 in the UV/chlorine system within 12 min of exposure (Table S7). In this system, the removal of BAC C12 was achieved by the combined action of ·OH and Cl·, which were produced from the photolysis of HOCl. pH also affected the removal of BAC C12. An increase in pH from 3.6 to 9.5 reduced the BAC C12 removal from 81.4 to 56.6%. Such a reduced removal rate at high pH is likely attributed to the less reactive OCl^- form of HOCl at higher pH above 7.6. Moreover, the quantum yield of HOCl ($\phi = 0.7$) is higher than that of OCl- ($\phi = 0.5$), resulting in more radical formation. Therefore, the generation of more reactive Cl· radicals is inhibited at high pH. Again, at high pH, the contribution of the ·OH radicals increased compared to Cl· as Cl· is more reactive with OH^- and forms selective and low oxidation potential ClOH· which further decomposes to form ·OH and Cl^-. Even though the redox potential of Cl· (2.41 V) is reported to be comparable to the redox potential of ·OH, the reported removal in UV alone and chlorine alone were 42% and 7%, respectively. When this study was further extended by Xiao et al. [65] to evaluate the BAC C12 degradation in a vacuum ultraviolet (VUV)/UV/chlorine system, it was found that, within 10 min of the experiment, chlorine alone could not degrade BAC C12, and UV showed only slight degradation (14%) (Table S8). However, UV/chlorine and VUV/UV showed moderate degradation for BAC C12 of 36–38%, and VUV/UV/chlorine exhibited the best degradation for BAC C12 of 58%. This is because the reaction of VUV photons with water produces ·OH radicals. As such, the degradation of BAC C12 was higher by VUV/UV/chlorine and UV/chlorine than without combining with chlorine.

$$O_3 + OH^- \rightarrow HO_2^{\cdot} + O_2^{\cdot-} \quad (8)$$

$$O_2^{\cdot-} + O_3 + H_2O \rightarrow {}^{\cdot}OH + 2\,O_2 + OH^- \quad (9)$$

Another study was conducted by Yu et al. [67] on BAC C12 in the O_3/UV system (Table S9). Under neutral to slightly acidic conditions, there was a significant increase in the degradation of BAC C12 from 18.6% in the presence of O_3 alone to 92.9% after 20 min of O_3/UV irradiation. This is because O_3 is efficiently degraded into ·OH, which reacts with BAC C12 substantially faster than molecular O_3. Under alkaline conditions, the degradation of BAC C12 was 98.2% due to the efficient production of ·OH from O_3 alone. However, the combined action of O_3 and UV (UV irradiance intensity = 3.53 mW•cm^{-2} Table 1) under alkaline conditions resulted in the highest removal (99.3%) due to the production of different radicals such as $HO_2^{\cdot}$, $O_2^{\cdot-}$, $O_3^{\cdot-}$ and ·OH. When O_3 dosage was increased from 0.37 g/h to 4.37 g/h, there was a significant increase in BAC C12 degradation from 19.1% to 96.7% without UV, but only a limited increase in degradation from 90.2% to 99.3% of BAC C12 under UV for 20 min. This is because a higher O_3 dosage gives rise to a higher O_3 concentration in the gas phase, and by Henry's law would result in a higher concentration of O_3 in an aqueous solution. This leads to higher production of ·OH and hence, faster degradation. However, under UV, ·OH would result in the reaction with excess O_3 to generate less oxidative species. A study by Hora & Arnold [21] further evaluated the extent of indirect photodegradation for BAC C12, BAC C14 and benzethonium chloride (BZT) in Mississippi River water with hydrogen peroxide (H_2O_2) (Table S2). However, no significant degradation was observed for BAC C12 and C14 when experiments were conducted by spiking H_2O_2, whereas BZT showed significant degradation in the presence of H_2O_2. The bimolecular rate constants (K_{OH}) for BAC C12, BAC C14 and BZT were 1.1×10^{10} M^{-1} s^{-1}, 1.2×10^{10} M^{-1} s^{-1} and 1.08×10^{10} M^{-1} s^{-1}, respectively.

3.4. Photocatalytic degradation

In addition to direct and indirect photodegradation, photocatalytic removal of QACs was studied in lab-scale studies. Serpone [57], for the first time, studied the photocatalytic degradation of benzyl tetradecyldimethyl ammonium chloride (BTDAC or BAC C14) and hexadecyltrimethyl ammonium bromide (CTAB or ATMAC C16) using TiO_2 catalyst and the removal of the QACs were evaluated through total organic carbon (TOC) removal (Table S10). TOC removal for BAC C14 and ATMAC C16 was 74.4% and 55.1%, respectively, at the end of 5 h. Although no measurements on the QACs were documented due to analytical challenges, the degradation of these cationic surfactants is considered slower than other surfactants due to the very slow photo-mineralization of the alkyl chain. Later, Miłosek et al. [46] evaluated the photocatalytic degradation of Tetraoctylammonium bromide (TOAB) using the same TiO_2 catalyst (Table S11). The half-life of TOAB was significantly lower in river water at 138 min compared to the in model solution at 578 min. This is because the NOM in river water acted as a photosensitizer, allowing for a series of radical reactions that resulted in quicker degradation of TOAB. The half-life of TOAB was also significantly lower in the presence of TiO_2 in anatase form of 62 min as compared to the in model solution. In addition to ·OH, the adsorption of TOAB onto the surface of TiO_2 due to electrostatic action also increased the degradation of TOAB. However, such adsorption is expected to be low at pH 6 – 7, as seen during the photocatalytic degradation of benzalkonium chloride (BKC) [40].

BKC concentration decreased slightly by 8.5% when left in contact

with TiO_2 for 30 min in the dark because of adsorption onto the catalyst surface. TiO_2 is slightly positively charged at pH 7, which does not favor the adsorption of cationic BKC due to electrostatic repulsion. Thus, it took around 180 min for the complete removal of BKC. To overcome the electrostatic repulsion between TiO_2 and cationic QACs, Suchitra et al. (2015) synthesized negatively charged activated carbon (AC) and TiO_2 composite (ACT) and studied the degradation of BKC (Table S12). Thus, incorporating a negative surface-charged AC on TiO_2 improved the interaction between ACT and positively charged BKC [60]. The point of zero charges (pHpzc) of TiO_2 and AC is 6.18 and 2.72, respectively. Therefore, an increase in the AC content in the ACT composite further increases the negative charge on the ACT composite, leading to high removal of cationic BKC in the aqueous solution. As a result, the photocatalytic degradation of BKC increased from 9.6% to 80.3% when the composition of AC in ACT increased from 0% to 100% under dark conditions. The increase in adsorption capacity within 1 h of the experiment was mainly attributed to increased AC surface area. Under UV exposure, BKC degradation increased significantly from 68.5% to 99.9% when the composition of AC increased from 0 to 10% within 1 h of the experiment. However, the removal of BKC was subsequently decreased and showed no significant effect as the composition of AC increased further to 100%. The degradation of BKC was lower with a 100% composition of TiO_2 as TiO_2 becomes positively charged when in contact with UV, and since BKC is cationic, it will be repelled away from the surface due to similar charges. AC plays an important role in the adsorption of BKC onto the TiO_2 surface, as hybridizing AC onto TiO_2 gives the catalyst surface a negative charge in addition to the highly favorable adsorption sites provided for BKC. This led to high degradation when the composition of AC was increased to 10%. The degradation of BKC subsequently decreased to an insignificant effect because the hybridization of TiO_2 onto AC obstructed the pores on the AC surface and led to a decrease in the degradation of BKC.

Kuźmiński et al. [33] further studied the photocatalytic degradation of cationic benzethonium chloride (BtCl) and anionic sodium dodecylbenzene sulfonate (NaDBS) in the presence of UV, O_3 and TiO_2 – P25 and TiO_2/N catalysts (Tables S13). Surface charge on the photocatalyst plays a major role in the photocatalytic activity of BtCl and NaDBS. pHpzc of TiO_2-P25 and TiO_2-N is 5.65 and 6.7, respectively. Under acidic conditions, anionic NaDBS adsorbed efficiently on the TiO_2-P25 and TiO_2-N with adsorption capacities of 140 and 196 mg/g, respectively. Similarly, under alkaline pH, cationic BtCl adsorbed on the TiO_2-P25 and TiO_2-N with adsorption capacities of 85 and 100 mg/g, respectively. As a result of the adsorption of QACs on the photocatalyst, the interaction between target QACs and generated reactive oxygen species (ROS) during the photocatalytic degradation process was significantly improved, leading to the degradation of BtCl and NaDBS. In this study, photocatalytic degradation of both QACs was conducted at pH 5.4, and it was observed that BtCl removal was higher using TiO_2-P25 than TiO_2-N, whereas NaDBS removal was higher using TiO_2-N than TiO_2-P25. This is likely because, at pH 5.4, TiO2-N has a more positive charge than TiO_2-P25, being more favorable in removing anionic NaDBS.

Under UV + TiO_2 – P25 and UV + TiO_2/N system, the degradation of BtCl increased significantly to 85–90% and 80–82%, respectively, as compared to UV only. Similarly, the UV + O_3 + TiO_2 – P25 and UV + O_3 + TiO_2/N systems had slightly higher degradation rates of 82–83% and 84–85%, respectively, compared to the UV + O_3 system. This is because the added catalyst has a high surface area, allowing BtCl to be adsorbed onto the surface, and subsequent surface oxidation increases the BtCl removal. It was also observed that the UV + TiO_2/N system had slightly lower degradation of BtCl as compared to the UV + TiO_2 – P25 system. This is because the high surface positive electrokinetic potential of TiO_2/N repels the cationic BtCl surfactant; this further decreases the oxidation efficiency and hence, results in slightly lower degradation rates.

In lab-scale studies, the photocatalytic degradation of QACs has been studied using TiO_2 catalysts or in combination with AC. However, the degradation rate of cationic surfactants is slower due to the slow photomineralization of the alkyl chain leading to the formation of several TPs, as discussed below with the help of computational analysis. Future research can focus on developing more effective photocatalysts to enhance the photocatalytic degradation of QACs where the effect of various factors, such as the concentration of QACs, pH, and reaction time, can be optimized.

3.5. Photodegradation pathway and computational analysis

3.5.1. Benzylalkyldimethyl ammonium compounds (BACs)

So far, limited research has been performed on the degradation pathways of a few QACs, such as BAC C12 or DDBAC and ATMAC C12 or DTAC. Hence, in this section phototransformation of remaining BACs and ATMACs are discussed with the help of computational analysis and phototransformation results published for BAC C12 and ATMAC C12.

3.5.2. Phototransformation of BAC C12 or DDBAC

Among BACs, the phototransformation of BAC C12 has only been studied extensively. The study by Huang et al. [25] on BAC C12 degradation by UV/chlorine oxidation reported five main TPs (Fig. 4, TP1 and TP2 pathways). The cleavage of the benzyl-nitrogen bond of DDBAC resulted in TP1 ($m/z = 214$), which, upon demethylation, formed TP1.1 ($m/z = 200$). The hydroxylation and hydrogen abstraction of TP1 resulted in TP 1.2 and TP1.3 ($m/z = 228$), respectively. Hydrogen abstraction of the alkyl chain through a hydroxyl radical followed by the reaction with dissolved oxygen in the solution formed TP2 ($m/z = 318$). TP1.3/2.1 is also reported to be produced from TP2 ($m/z = 318$) via pathway 2.1 through the cleavage of the benzyl-nitrogen bond.

During BAC C12 degradation in the UV/PS/Cu^{2+} system, Lee et al. [34] identified fifteen main oxidation products (Fig. 4, TP3 to 6 pathways). The degradation pathways mainly included hydrogen abstraction resulting in TP3, the addition of a hydroxyl molecule resulting in a series of products such as TP4, TP4.1, TP4.2 and TP4.1.1/4.2.1, and the cleavage of a benzyl-nitrogen bond resulting in TP6. Hydrogen abstraction of TP3 formed TP3.1. Further hydroxylation of TP6 formed TP6.1 and TP6.2 and then TP6.1.1/6.2.1, TP6.1.2 and TP6.2.2. TP5 was produced via the central fission of the C_{alkyl}-N bond of BAC C12. Although not reported in the study, the detection of TP5.1 suggested an esterification reaction between benzenecarboxylic acid and benzaldehyde.

Further degradation of BAC C12 in a VUV/UV/chlorine system, Xiao et al. [65] identified six TPs (Fig. 4, TP7 to 10 pathways). Similar to previous studies, the degradation pathways mainly involved hydrogen abstraction, hydroxylation, and cleavage of the C-N bond. TP7 was formed primarily by adding a carbonyl group to BAC C12. TP8 was formed by displacing an H atom with the hydroxyl group and then with the hydroxyl group on benzene or alkane. Further oxidation or substitution of TP7, TP8 and TP9 formed TP7.1/8.1 and TP7.2/9.1 with hydroxyl groups at different positions. TP10 was derived through the cleavage of the C-N bond in DDBAC, which might have further undergone oxidation and substitution with carbonyl and hydroxyl groups to produce TP10.1 and then TP10.2.

The study by Lee et al. [35] on BAC C12 degradation by UV/PS identified five TPs (Fig. 4, TP11 to 13 pathways). The degradation occurred mainly via two pathways, the first being an attack at a hydrophobic part of the compound and the second on the hydrophilic part. The hydrophobic part was started by the addition of·OH, which formed TP11. The hydrophilic route was initiated by removing the benzyl substituent to form a carboxylic acid that resulted in TP13 ($m/z = 214$), TP12.1 ($m/z = 228$) and TP13.1 ($m/z = 200$), probably through quinonization. In addition, hydrogen abstraction of DDBAC produced TP12 ($m/z = 318$), which then formed TP12.1 ($m/z = 228$) after cleavage of the benzyl-nitrogen bond. Furthermore, two mechanisms are responsible for the hydroxylation of the aromatic ring: an electrophilic attack

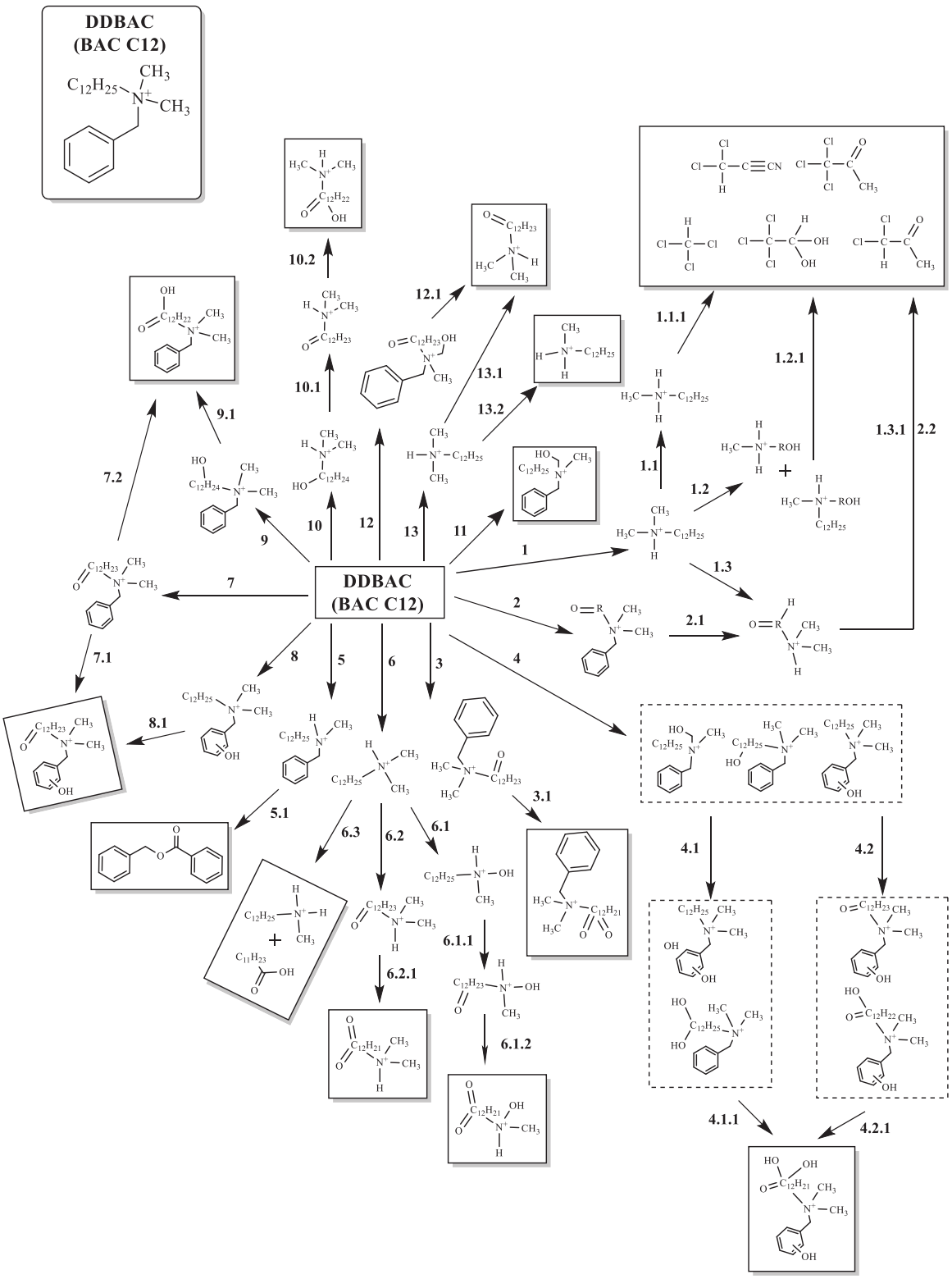

Fig. 4. Photo transformation pathway for BAC C12 reported in the literature.

by·OH and direct electron transfer from an aromatic compound to $SO_4^{\cdot-}$ to produce a radical cation that would hydrolyze to form·OH.

3.5.3. *Structure optimization for BACs*

Except for BAC12, no studies have reported the phototransformation of other BACs, underscoring the need to explore the photodegradation pathway for structurally similar BACs using computational calculations. Fig. 1 illustrates the optimized numbered structure of BACs. Due to their similar molecular structure, BAC C14–18 are expected to lead to similar if not identical degradation pathways as BAC C12. The computational data presented herein provide insights into the degradation products of BAC C12 but also help predict the degradation paths for other BACs.

Frontier Molecular Orbitals (FMO) characterization is a widely used tool to understand the reactivity of molecules based on the shape of

HOMO and LUMO orbitals and the atoms that participate in them. In this context, the HOMO orbital represents the portion of a molecule in which electrophilic attacks could occur due to the electron-donating character of the atoms located on it. Conversely, those atoms at the LUMO orbital present an electron-withdrawing character; thus, nucleophilic attacks are highly susceptible in this moiety. Such theoretical calculations [51, 61] were previously applied in photodegradation studies. Fig. 2 shows the representation of the HOMO and LUMO orbitals for selected QACs under study at the M06–2X/6–311 G(d,p) level of theory. As can be seen, the representation of the FMO in BACs compounds is quite similar. Chlorine atoms, along with carbon and hydrogen atoms pointing toward the Cl anion, take part in the HOMO orbital of BAC C12, C14, C16 and C18. On the other hand, the benzyl group and nitrogen atoms of the previously mentioned compounds take part in the LUMO orbitals. This behavior follows the N atom's cationic character and the anionic nature of the Cl atoms present in QACs. These results can be further explained by analyzing the effect of the cationic N atom on the benzyl group. The presence of positively charged N atoms alters the electronic environment of the benzyl moiety and withdraws electron density from it to counteract the positive charge. The net effect is that both the nitrogen atom and the benzyl group have low electron density. This similar behavior encountered in BACs further strengthens our prediction that computational analysis may provide insights into the degradation pathways of the less studied BAC C14-C18.

Single Point calculations at UM06–2X/6–311 G(2df,2pd) were carried out to determine the condensed nucleophilic, electrophilic, and radical Fukui functions based on ADCH population analysis and shown in Fig. 3. It was found that BAC C12 (Fig. 3a) and BAC C16 (Fig. 3c) have similar Fuki functions. Similar behavior is also seen between BAC C14 and BAC C18. These results could be explained by their similar structures and FMO shape, with the benzene moiety pointing toward the chlorine atom in BAC C14 and C18 and the cationic nitrogen atom in BAC C12 and C16. BAC C12 and C16 have no significant changes in the electrophilic Fukui function, with most values around 0 u.a. On the other hand, carbons-5, 9, 10, and 11, along with hydrogens-31–37 for BAC C12 and hydrogens-35–41 for BAC C16, are found to be the most susceptible sites toward nucleophilic attacks. Even the radical attack can occur at the same locations, carbon-11 and hydrogens-33, 34 for BAC C12 and hydrogens-37, 38 for BAC C16, experiencing the highest radical values. It is important to note that the most reactive hydrogen atoms' electronic energy values of BAC C12 match those of BAC C16 (Fig. 1).

3.5.4. Phototransformation of other BACs from a computational perspective

The appearance of very reactive atoms in the hydrophilic and hydrophobic parts of BAC C12 follows the experimental observations collated in this paper, which identified TPs involving both moieties taking part in the degradation pathways. For example, the abstraction of hydrogen atoms through radical-based reactions of the alkyl moiety followed by hydroxylation or addition of keto groups was essential, as reported by many studies (Fig. 4). These reactions can be explained with the aforementioned computational results, which suggest the participation of hydrogens 31–37 of BAC C12 in radical and nucleophilic-based reactions (TP9, TP9.1, TP3, TP3.1, and TP4).

These -OH and keto-containing degradation products can be further degraded by similar reactions but in the benzyl moiety (TP8.1, TP4.1, and TP4.2). In this case, the participation of carbon-5, 9, 10, and 11 of BAC C12 in hydrogen displacement reactions is of great importance. Furthermore, the nucleophilic character of these atoms sustains their participation in direct electron transfer processes with radicals from the environment to produce radical cations, which are further hydrolyzed to obtain -OH-containing benzyl groups. These electron transfer pathways were proposed in the degradation study of BAC C12 by UV/PS. Cleavage of the C-N bond was also found to be one of the most common reactions in the degradation mechanism of BAC C12 in all studies reviewed in this work. Participation of carbon 5, which is directly attached to the cationic nitrogen and constitutes one of the most susceptible sites toward radical and nucleophilic attacks, may lead to the formation of degradation products upon cleavage of the C-N bond (TP6, TP1 and TP6/13). These reactive degradation products may be further hydrolyzed at the alkyl moiety through radical-based hydrogen abstraction reactions, as reported elsewhere [35]. Degradation pathways concerning BAC C16 are less well studied than those for BAC C12. As demonstrated by the FMO characterization and the behavior of Fukui functions, BAC C12 and C16 possess similar structures and local electronic properties; thus, the degradation pathway of BAC C16 might also be similar to that of BAC C12. However, the degradation process may need harsher conditions as BAC C16 is more stable than BAC C12 due to its longer alkyl chain [49], as seen in Fig. 1. Hence, hydrogen displacement reactions at the hydrophilic and hydrophobic parts and C-N bond cleavage through radical and nucleophilic reactions could be the most critical processes in BAC C16 degradation.

For BAC C14 and C18, carbon-6 and 11 constitute the most reactive sites toward electrophilic attacks. Carbon-7, 8 and 9 and hydrogen-33–39 for BAC C14 and hydrogens-37–43 for BAC C18 possess the highest condensed nucleophilic Fukui function values. Although these atoms are equivalent in both structures (Fig. 1), carbon-7 and 11, along with hydrogen-34, 35 and 36 in BAC C14 and hydrogen-37, 38 and 39 in BAC C18, are the most susceptible site where radical attacks can occur. Like BAC C16, there is insufficient experimental data on the degradation pathway of BAC C14 and C18; thus, the presented computational results could assist in help suggesting their possible degradation products. Due to the resemblance between BAC C14-C18 and BAC C12 in their local electronic properties and FMO, it is expected that the degradation pathways of these QACs are similar to that of BAC C12. However, the susceptibility of reactive sites, namely carbon-6 and 11, toward electrophilic reactions may lead to a hydroxylation with the hydroxyl radicals. As discussed in the previous section for BAC C12, this reaction has already been verified and constitutes a common way to hydrolyze benzene moieties [36].

3.6. Alkyltrimethyl ammonium compounds (ATMACs)

3.6.1. Phototransformation of ATMAC C12 or DTAC

While most of these studies only looked at the degradation of BAC C12, a study by Lee et al. [34] reported the degradation of ATMAC C12 in UV/PS/Cu^{2+} for the first time and found nine main oxidation products (Fig. 5). Like BACs, the HOMO orbital of ATMAC C12 is localized at the chlorine and carbon atoms (carbon 3 and 4), pointing toward the anionic part of the molecule (Fig. 1). Nitrogen, the remaining methyl group, and carbon-5 and 6 participate in the LUMO orbital of ATMAC C12 (Fig. 2). Nucleophilic, electrophilic and radical values of ATMAC C12 were also determined and are shown in Fig. 3e. Like BAC C12 and BAC C16, electrophilic values for ATMAC C12 were found to be around 0 u.a for most atoms. Concerning the nucleophilic and radical Fukui functions, hydrogen-17, 19, 21, 25–27 are the most susceptible sites toward nucleophilic and radical-based reactions. These hydrogen atoms are located either in the methyl or dodecyl group, as shown in Fig. 1. Single and multiple radical-based hydrogen displacements can yield degradation products containing -OH and keto groups, as shown in Fig. 5. C-N bond cleavage, a common reaction in the ATMAC C12 degradation process, can not be predicted by Fukui functions or FMO characterization. The cleavage of the C-H or C-C bond gave TP7, which, after hydroxylation and hydrogen abstraction, produced TP6 and TP4. TP3, TP2 and TP5 were formed after successive hydroxylation on the long alkyl chain (Fig. 5). Likewise, TP1 was formed via cleavage of central fission of the C_{alkyl}-N bond. TP9 was produced through cleaving the C-C bone and would eventually give TP8.

3.6.2. Structure optimization and phototransformation of other ATMACs

Similar to the BACs C14–18, no experimental work has been carried out on other ATMACs C14–18 to determine their degradation pathways.

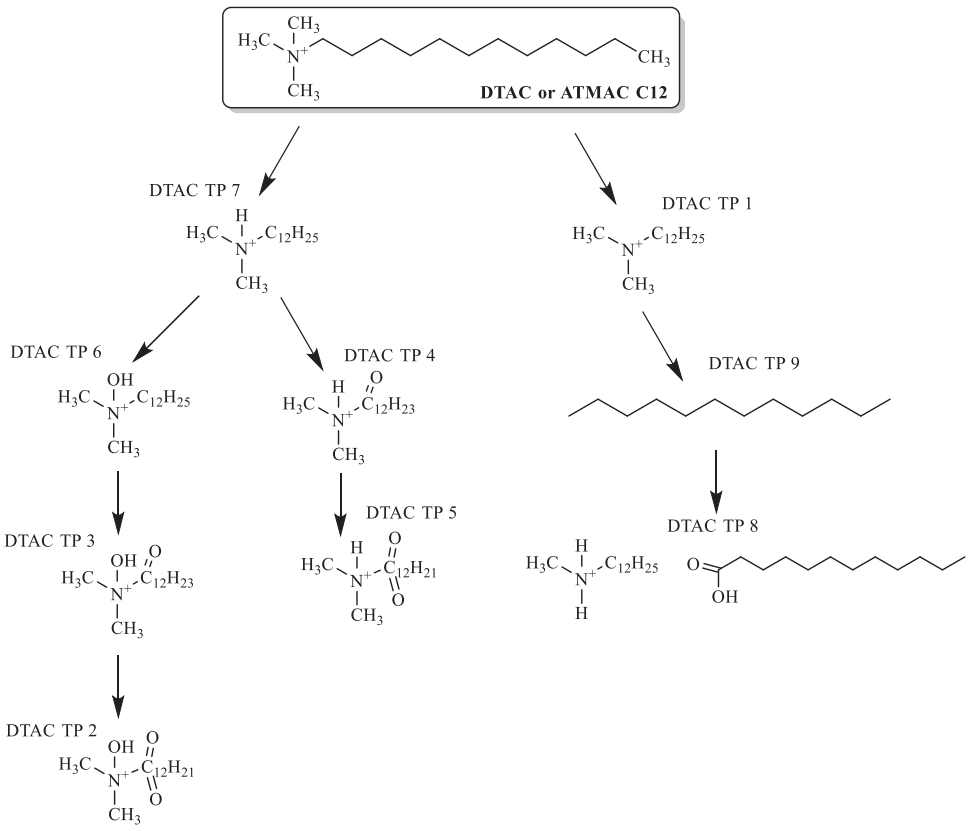

Fig. 5. Proposed degradation pathway for DTAC in UV/PS/Cu^{2+} (Reproduced with permission from Lee et al. [34]).

Computational studies are, therefore, crucial for understanding their reactivities and properties. In this context, similar quantum chemistry calculations on larger members of ATMACs, namely ATMAC C14 and ATMAC C18, were performed to shed light on their possible transformation products. Fig. 2f and g show the representation of FMOs for ATMAC C14 and ATMAC C18, respectively.

Like ATMAC C12, the HOMO of ATMAC C14 is mainly located in the chlorine atom and C-H bonds pointing toward the negatively charged side of the molecule, while nitrogen and carbon-5 and 6 take part in the LUMO. Concerning the values for electrophilic Fukui function, most atoms in ATMAC C14 are found to be around 0 u.a., similar to ATMAC C12 and BACs included in this work. Regarding nucleophilic and radical Fukui functions, hydrogens-20, 22, 24, 26, and 31 constitute the more reactive sites toward nucleophilic and radical attacks. These reactivity features match those found in ATMAC C12, as seen in Fig. 1e.

As shown in Fig. 2g, FMOs representations for ATMAC C18 do not match those found for the remaining ATMACs included in this study. However, local properties modeled in this work, such as condensed Fukui functions, are very similar to ATMAC C12. Hydrogens located in the alkyl chain, as well as methyl groups bound to the cationic nitrogen atom, are the most active sites where nucleophilic and radical reactions can occur. Therefore, possible transformation products from the degradation of ATMAC C14 and C18 are expected to be similar or identical to those reported for ATMAC C12. Reactions ranging from radical-based hydrogen displacement and abstraction to hydroxylation, driven by the reactive sites mentioned in section 6.2.1 and elucidated in Fig. 5, constitute plausible pathways in the degradation of ATMAC C14 and C18.

3.6.3. *Toxicity posed by degradation products*

So far, only three studies have reported the toxicity posed by a few QACs TPs. Huang et al. [25] studied the toxicity of BAC C12 and their TPs after UV, chlorine and UV-chlorine treatment based on the inhibition of luminescent bacteria, *Photobacterium phosphoreum*. At the beginning of the experiment, bacteria were inhibited by BAC C12 at an initial concentration of 10 mg/L. A similar observation was noticed after the chlorination, as BAC C12 was not degraded during the chlorination treatment alone (Table S7). However, treatment with UV and UV/chlorine decreased DDBAC toxicity, i.e., the inhibition ratio to 33% and 9%, respectively, after reaction for 120 min, showing that UV/chlorine was a more effective detoxification method than UV or chlorine alone. Looking deeper into the detoxification via UV/chlorine, the inhibition ratio dropped to 26% after the first 60 min and decreased to 9% by 120 min. The results obtained in the first 60 min suggested the association of toxicity with BAC C12 TPs but also that it can be decreased through BAC C12 removal. The generation of toxic TPs can also be speculated as there was residual toxicity after the complete removal of BAC C12. However, the continued detoxification in the next 60 min further suggests the degradation of toxic TPs. Overall, UV/chlorine can effectively degrade the parent compound and detoxify BAC C12.

Later, Lee et al. [35] reported toxicity for *Vibrio fisheri* during BAC C12 degradation using a UV/PS system (Table 2). After 15 min of reaction, the acute toxicity to *V. fisheri* decreased from 0.62 to 0.3 due to UV/PS oxidation of BAC C12. The residual toxicity in the sample was detected after 10 min, even when BAC C12 was completely degraded during UV/PS oxidation. Thus, the possible toxicity could be due to the TPs formed during BAC C12 degradation in the UV/PS system, and such TPs could be more toxic than BAC C12, as shown in Table 2. Apart from BAC C12, an attempt was made by Lee et al. [36] to study the acute toxicity of ATMAC C12 and their TPs obtained from the UV/PS system based on the inhibition of luminescent bacteria (Table 3, Table S4). The samples were exposed to luminescent bacteria at 20 °C for 15 min. The toxicity of ATMAC C12 significantly decreased from 0.75 to 0.49 in the UV/PS system at a UV dose of 87 mJ/cm^2 and was completely detoxified

Table 2
Acute and chronic toxicity of BAC C12 and their degradation products (Reused with permission from [35]).

Name	Structure	*Vibrio fisheri*	ECOSAR							
			Fish			Daphnia		Green algae		Oral Rat
		L (E)C_{50}	Log	96 h LC_{50}	ChV	48 h LC_{50}	ChV	96 h EC_{50}	ChV	LD_{50}
DDBAC	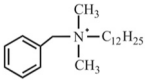	0.3	2.93	40.97	4.43	25.34	3.14	26.91	8.53	934.7
TP 1-1	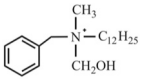	-	1.46	798.91	73.66	431.69	36.68	261.99	61.44	2458.03
TP 1-2	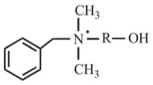	-	1.46	798.91	73.66	431.69	36.68	261.99	61.44	1501.22
TP 2	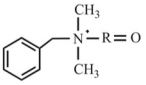	-	1.44	35.82	6.77	76.48	10.03	102.77	32.85	787.59
TP 3	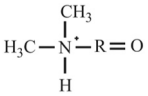	-	1.18	34.93	7.29	84.7	10.60	107.43	32.47	N/A
TP 4	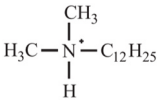	-	2.67	43.80	4.61	26.46	3.07	25.49	7.67	N/A
TP 5	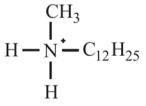	-	2.13	126.94	12.60	72.92	7.34	56.99	15.31	N/A

[a]LC_{50} represents Half Lethal Concentration, Unit = mg/L
[b]EC_{50} represents Half Effective Concentration, Unit = mg/L
[c]ChV, Chronic Value, represents chronic toxicity. ChV is defined as the geometric mean of the no observed effect concentration and the lowest observed effect concentration, Unit = mg/L
[d]LD_{50} represents Half Lethal Dose, Unit = mg/kg

Table 3
Basic toxicities results of ATMAC C12 through ECOSAR program (Reused with permission from [36]).

Organism	End point	Predicted Conc. (mg/L)
Fish (96-hr)	LC_{50}^{a}	1086.914
Daphnid (48-hr)	LC_{50}^{a}	574.293
Green Algae (96-hr)	EC_{50}^{b}	317.67
Fish	ChV[c]	97.593
Daphnid	ChV[c]	45.838
Green Algae	ChV[c]	70.869

at a high UV dose of 1305 mJ/cm^2. Thus, UV/PS systems operating at high UV fluence could effectively detoxify parent DTAC and its TPs.

The toxicity of QACs and their TPs is a growing concern due to their widespread use in various applications. Hence, more research in this direction must be conducted.

3.6.4. Comparison of different AOPs for the treatment of QACs

In this review, UV/PS, UV/Cl$^{\cdot}$, UV/O_3, UV/H_2O_2, and UV-assisted photocatalysis are discussed for treating QACs with a focus on the BAC 12 and ATMAC 12 (Table 1 and Table 4). Among several treatment techniques, in the UV/PS, UV/PS/Cu^{2+}, O_3, and UV/O_3 systems, QACs are removed from 90 to 99%, suggesting these techniques are suitable for QACs removal. However, for practical feasibility, it is also essential

Table 4
% Removal of ATMAC C12 and BAC C12 during various AOPs.

Treatment systems	% Removal		
	DTAC (ATMAC 12)	DDBAC (BAC 12)	BACs (% TOC removal)
UV	Barely occurred [34]	14-42 [25,35,65]	10-15 [33]
PS	Barely occurred [34]	19 [35]	-
Cl	-	7 [25]	-
UV/PS	65-91 [34,36]	66-90 [34,35]	-
UV/Cl	-	36-65 [25,65]	-
PS/ Cu^{2+}	5 [34]	4 [34]	-
UV/PS/Cu^{2+}	96.2 [34]	98.5 [34]	-
O_3	-	96.7 [67]	20-25 [33]
UV/O_3	-	99.3 [67]	75-80 [33]
UV/O_3/TiO_2	-	-	82-85 [33]

to look into the energy consumption of each treatment option and the residual toxicity posed by the transformation products. It is reported that the electrical energy per order (EEO) required in UV/PS is higher than in UV/H_2O_2 [11,31]. However, adding Fe^{2+} in UV/H_2O_2 reduces EEO [11]. Instead of UV light, the presence of the Fe^{2+}/ H_2O_2 during the Fenton process can significantly reduce the production cost of ·OH and subsequent organic pollutant removal. However, a low operating pH of ~3 and recovery of Fe^{2+}/Fe^{3+} from the aqueous system after treatment pose significant challenges [54]. It is also reported that the EEO cost of the UV/Cl^- system is less than 50% of the cost required for the UV/H_2O_2 system [11].

Compared to all other AOPs, UV/Cl^- exhibits greater selectivity towards the contaminants due to forming reactive chlorine species (RCS) and is primarily effective against organic contaminants with electron-donating groups [19]. However, it has a higher potential for generating disinfection by-products (DBPs) in real wastewater than other AOPs. Therefore, from a toxicity point of view, UV/Cl^- demonstrates more toxicity in some instances when contrasted with the ·OH forming UV/H_2O_2 system [19,37].

In the UV/PS system, a substantial amount of PS is required to generate $SO_4^{\cdot-}$ $SO_4^{\cdot-}$, being more stable than ·OH, in an aqueous system, exhibits greater selectivity for removing organic pollutants [63]. PS is an oxidant with a high oxidation potential that persists in the system post-treatment, potentially inducing toxicity in the aqueous environment. To address this concern, the UV/PS system necessitates post-treatment steps to eliminate PS from the aqueous system, which questions its economic feasibility.

UV light and visible light-assisted photocatalysis exhibit notable limitations in recovering nano-size catalysts from aqueous solutions after treatment [32,63]. The leaching of nanoparticles from the aqueous system can be mitigated by immobilizing the catalyst on an inert surface. However, this approach introduces challenges related to the cost of nanoparticle production and recyclability, potentially reducing effective surface area and mass transfer, thereby affecting removal efficiency.

In addition, the presence of natural organic matter (NOM) in secondary wastewater poses a significant obstacle as it functions as a scavenger for reactive oxygen species (ROS), inhibiting the efficient removal of QACs. The scale-up of technology faces challenges related to the penetration of light intensity, influencing the overall effectiveness of the process. Despite these challenges, photocatalysis and UV/H_2O_2 offer a significant advantage in terms of low disinfection by-product (DBP) formation.

It is crucial to acknowledge that various AOPs present advantages and disadvantages when removing QACs. Thus, each AOP must be carefully considered and applied based on the specific characteristics of the water or wastewater matrices where QACs are present together with other ECs, the treatment goals, and the environmental context to ensure optimal efficiency and minimal drawbacks. Suggestions for future research include:

1. Explore additional classes of QACs such as DADMACs and QACs of more (multi-QAC, poly-QAC) charged nitrogen atoms for their environmental and human toxicity and assess the efficacy of removal and treatment methods.
2. Shift the focus from lab-scale studies to investigations conducted in real-world wastewater treatment plants when exploring AOPs for QAC removal.
3. Investigate QACs TPs and their toxicity to gain a more comprehensive understanding.
4. Consider hybrid systems such as UV/PS or UV/H_2O_2 that integrate AOPs with other treatment methods, particularly when UV is applied, for more effective QAC removal and degradation.
5. Develop cost-effective AOPs that require minimal volumes of chemicals and have low operation and installation costs.

4. Conclusions

While direct photolysis is a significant mechanism for the natural attenuation of several ECs, based on the limited research conducted, QACs are found to be resistant to direct photodegradation in the laboratory or natural environment due to their stable structure. Therefore, researchers have focused on studying the fate of QACs during indirect photodegradation and photocatalytic degradation to develop effective strategies for their removal from water bodies. The studies critically reviewed and discussed in this paper demonstrate that the degradation of QACs can be improved through synergistic effects between different treatment systems. The combination of UV and H_2O_2, UV/PS, UV/PS/Cu^{2+}, UV/chlorine, VUV/UV/chlorine, and O_3/UV systems all show promising results for the degradation of QACs. These treatment systems produce highly reactive radicals such as ·OH, $SO_4^{\cdot-}$ and ·Cl, rapidly reacting with the QACs, leading to their degradation. The photocatalytic degradation of QACs has also been studied in laboratory-scale experiments. TiO_2 catalyst has been shown to be effective in degrading different types of QACs, such as BTDAC, CTAB, TOAB, BKC and BtCl, in different environments, including laboratory model solutions and river water. Hybridization of activated carbon onto TiO_2 also increased the photocatalytic degradation of BKC. UV and O_3 were also shown to have synergistic effects in degrading BtCl, with the addition of TiO_2 catalyst leading to higher degradation rates. The findings of these studies provide insights into potentially viable technologies that can be used to remove QACs during water and wastewater treatment, and further research can explore their effectiveness at larger scales. Additional research is necessary to optimize the treatment conditions for different QACs and to evaluate the long-term effects of these treatments on the environment.

Using a computational approach has shed light on the degradation pathway of QACs. For BKC, benzyl dimethyl amine was found to be degraded into ammonia through two pathways. Similarly, the degradation pathways of BAC-12 in different systems were mainly involved in hydrogen abstraction, hydroxylation, and cleavage of the C-N bond. ATMAC C12 was also found to be degraded through similar mechanisms, with the cleavage of the C-H or C-C bond being the primary pathway. The results of these studies are important as QACs are widely used as disinfectants in many industries, and their degradation products may have adverse effects on the environment and human health.

In conclusion, the toxicity of QACs and their TPs have been studied in only a few instances. However, the results from these studies suggest that QACs TPs can be more toxic than the parent compounds. Moreover, the toxicity of the TPs can persist even after the complete degradation of the parent compounds, indicating the importance of studying and understanding the TPs formed during the degradation of QACs. The studies also suggest that UV/chlorine and UV/PS systems can effectively degrade the parent compounds and detoxify QACs. However, the efficiency of detoxification may depend on the dosage of UV and the treatment time. Therefore, it is essential to optimize the treatment conditions to ensure the complete detoxification of QACs and their TPs.

Overall, there is a need for more comprehensive studies to evaluate the toxicity of QACs and their TPs under different environmental conditions and to determine the best treatment options to mitigate the risks associated with QACs in the environment. Hence, a better understanding of the degradation pathways and TPs of QACs is essential to develop effective strategies for their disposal and management. Further research is required to fully understand the environmental fate and impact of these compounds, especially in aquatic environments where they are commonly found.

Environmental implication

Direct photolysis, a natural attenuation mechanism, is not effective for QACs due to their stable structure. However, indirect photodegradation and photocatalytic degradation can effectively remove

QACs from water bodies. The combination of different treatment systems, such as UV and H_2O_2, UV/PS, UV/PS/Cu^{2+}, UV/chlorine, VUV/UV/chlorine, and O_3/UV, have shown positive results in degrading QACs. This comprehensive review further highlights the toxicity of QACs and their transformation products is a concern, and additional research is needed to evaluate toxicity under different conditions and determine optimal treatment options for mitigating risks.

CRediT authorship contribution statement

Mohapatra Sanjeeb: Conceptualization, Data curation, Formal analysis, Funding acquisition, Investigation, Methodology, Supervision, Writing – original draft, Writing – review & editing. **Xian Jovina Lew Li:** Writing – original draft, Writing – review & editing. **Gálvez-Rodríguez Andy:** Data curation, Formal analysis, Methodology, Software, Writing – original draft, Writing – review & editing. **Ekande Onkar Sudhir:** Formal analysis, Writing – original draft, Writing – review & editing. **Drewes Jörg E.:** Supervision, Writing – review & editing. **Gin Karina:** Funding acquisition, Project administration, Supervision, Writing – review & editing.

Declaration of Competing Interest

The authors declare that they have no known competing financial interests or personal relationships that could have appeared to influence the work reported in this paper.

Data availability

Associated data can be found in the SI.

Acknowledgment

This research is funded by the National Research Foundation (NRF), Prime Minister's Office, Singapore, under its Campus for Research Excellence and Technological Enterprise (CREATE) program (Intra-CREATE Thematic Project NRF2019-THE001–0003), administered by the NUS Environmental Research Institute (NERI), Singapore. Ulises J. Jauregui, Raphael Pasquier, Jacques Laminie, and Pascal Poullet are also acknowledged for their support to the computational calculation facilities at Wahoo and the cluster of the Centre Commun de Calcul Intensif of the Universite des Antilles, Guadeloupe, France. This work is further co-funded by the European Union. Views and opinions expressed are however those of the author(s) only and do not necessarily reflect those of the European Union or the European Commission. Neither the European Union nor the granting authority can be held responsible for them.

Appendix A. Supporting information

Supplementary data associated with this article can be found in the online version at doi:10.1016/j.jhazmat.2024.133483.

References

[1] Akimitsu, N., Hamamoto, H., Inoue, R.I., Shoji, M., Takemori, K., Hamasaki, N., Sekimizu, K., 1999. Increase in resistance of methicillin-resistant Staphylococcus aureus to β-lactams caused by mutations conferring resistance to benzalkonium chloride, a disinfectant widely used in hospitals. Antimicrob Agents Chemother 43 (12), 3042–3043. https://doi.org/10.1128/aac.43.12.3042.

[2] Alvareda, E., Denis, P.A., Iribarne, F., Paulino, M., 2016. Bond dissociation energies and enthalpies of formation of flavonoids: A G4 and M06-2X investigation. Comput Theor Chem 1091, 18–23. https://doi.org/10.1016/J.COMPTC.2016.06.021.

[3] Arnold, W.A., Blum, A., Branyan, J., Bruton, T.A., Carignan, C.C., Cortopassi, G., Datta, S., Dewitt, J., Doherty, A.-C., Halden, R.U., Harari, H., Hartmann, E.M., Hrubec, T.C., Iyer, S., Kwiatkowski, C.F., Lapier, J., Li, D., Li, L., Muñ Iz Ortiz, J.G., Salamova, A., Schettler, T., Seguin, R.P., Soehl, A., Sutton, R., Xu, L., Zheng, G., 2023. Quaternary Ammonium Compounds: A Chemical Class of Emerging Concern. Environ Sci Technol 57, 7645–7665. https://doi.org/10.1021/acs.est.2c08244.

[4] Arulmozhiraja, S., Kolandaivel, P., 1997. Condensed Fukui function: Dependency on atomic charges. Mol Phys 90 (1), 55–62. https://doi.org/10.1080/002689797172868.

[5] Buffet-Bataillon, S., Tattevin, P., Bonnaure-Mallet, M., Jolivet-Gougeon, A., 2012. Emergence of resistance to antibacterial agents: The role of quaternary ammonium compounds - A critical review. Int J Antimicrob Agents 39 (5), 381–389. https://doi.org/10.1016/j.ijantimicag.2012.01.011.

[6] Chaves, R.D., Kumazawa, S.H., Khaneghah, A.M., Alvarenga, V.O., Hungaro, H.M., Sant'ana, A.S., 2024. Comparing the susceptibility to sanitizers, biofilm-forming ability, and biofilm resistance to quaternary ammonium and chlorine dioxide of 43 Salmonella enterica and Listeria monocytogenes strains. Food Microbiol 117, 104380. https://doi.org/10.1016/j.fm.2023.104380.

[7] Clara, M., Scharf, S., Scheffknecht, C., Gans, O., 2007. Occurrence of selected surfactants in untreated and treated sewage. Water Res 41 (19), 4339–4348. https://doi.org/10.1016/j.watres.2007.06.027.

[8] Clinic, E.M., 2015. Quaternary Ammonium Compounds in Cleaning Products: Health & Safety Information for Health Professionals. Selikoff Cent Occup Health: -Mt Sinai 1–9.

[9] Ding, W.H., Liao, Y.H., 2001. Determination of alkylbenzyldimethylammonium chlorides in river water and sewage effluent by solid-phase extraction and gas chromatography/mass spectrometry. Anal Chem 73 (1), 36–40. https://doi.org/10.1021/ac000655i.

[10] Ebadi, A., Noei, M., 2017. Evaluating Minnesota 2006 density functionals against some challenging problems in DFT. J Mol Model 23 (2), 1–7. https://doi.org/10.1007/S00894-017-3213-3/METRICS.

[11] Farzanehsa, M., Vaughan, L.C., Zamyadi, A., Khan, S.J., 2023. Comparison of UV-Cl and UV-H2O2 advanced oxidation processes in the degradation of contaminants from water and wastewater: A review. Water Environ J.

[12] Fernández, P., Alder, A.C., Suter, M.J.F., Giger, W., 1996. Determination off the quaternary ammonium surfactant ditallowdimethylammonium in digested sludges and marine sediments by supercritical fluid extraction and liquid chromatography with postcolumn ion-pair formation. Anal Chem 68 (5), 921–929. https://doi.org/10.1021/ac9505482.

[13] Frisch, M.J., Trucks, G.W., Schlegel, H.B., Scuseria, G.E., Robb, M.A., Cheeseman, J.R., & Fox, D.J. (2009). Gaussian 09 (Verion Revision E. 01). Wallingford, CT.

[14] Frantz, A.L., 2023, Chronic quaternary ammonium compound exposure during the COVID-19 pandemic and the impact on human health 15, 199–206. https://doi.org/10.1007/s13530–023-00173-w.

[15] Fuentealba, P., Pérez, P., Contreras, R., 2000. On the condensed Fukui function. J Chem Phys 113 (7), 2544–2551. https://doi.org/10.1063/1.1305879.

[16] Gálvez-Rodríguez, A., Ferino-Pérez, A., Rodríguez-Riera, Z., Rodeiro Guerra, I., Řeha, D., Minofar, B., Jáuregui-Haza, U.J., 2022. Explaining the interaction of mangiferin with MMP-9 and NF-κβ: a computational study. J Mol Model 28 (9), 1–16. https://doi.org/10.1007/S00894-022-05260-2/METRICS.

[17] Germani, R., Bragetta, M., Tiecco, M., Alabed, H.B.R., Giacco, T.Del, 2023. Photocatalytic degradation of carbendazim by TiO 2 in aqueous medium: effect of bromide in improving process performance. SSRN. https://doi.org/10.2139/ssrn.4494262.

[18] Gonzalez, M., Jégu, J., Kopferschmitt, M.C., Donnay, C., Hedelin, G., Matzinger, F., Velten, M., Guilloux, L., Cantineau, A., de Blay, F., 2013. Asthma among workers in healthcare settings: role of disinfection with quaternary ammonium compounds. Clin Exp Allergy 44 (3), 393–406. https://doi.org/10.1111/CEA.12215.

[19] Guo, K., Wu, Z., Chen, C., Fang, J., 2022. UV/chlorine process: an efficient advanced oxidation process with multiple radicals and functions in water treatment. Acc Chem Res 55 (3), 286–297.

[20] Heederik, D., 2014. Cleaning agents and disinfectants: Moving from recognition to action and prevention. Clin Exp Allergy 44 (4), 472–474. https://doi.org/10.1111/cea.12286.

[21] Hora, P.I., Arnold, W.A., 2020. Photochemical fate of quaternary ammonium compounds in river water. Environ Sci: Process Impacts 22 (6), 1368–1381. https://doi.org/10.1039/d0em00086h.

[22] Hora, P.I., Pati, S.G., McNamara, P.J., Arnold, W.A., 2020. Increased Use of Quaternary Ammonium Compounds during the SARS-CoV-2 Pandemic and Beyond: Consideration of Environmental Implications. Environ Sci Technol Lett 7 (9), 622–631. https://doi.org/10.1021/acs.estlett.0c00437.

[23] Hostaš, J., Řezáč, J., Hobza, P., 2013. On the performance of the semiempirical quantum mechanical PM6 and PM7 methods for noncovalent interactions. Chem Phys Lett 568–569, 161–166. https://doi.org/10.1016/J.CPLETT.2013.02.069.

[24] Hrubec, T.C., Seguin, R.P., Xu, L., Cortopassi, G.A., Datta, S., Hanlon, A.L., Lozano, A.J., McDonald, V.A., Healy, C.A., Anderson, T.C., Musse, N.A., Williams, R.T., 2021. Altered toxicological endpoints in humans from common quaternary ammonium compound disinfectant exposure. Toxicol Rep 8, 646–656. https://doi.org/10.1016/j.toxrep.2021.03.006.

[25] Huang, N., Wang, T., Wang, W.L., Wu, Q.Y., Li, A., Hu, H.Y., 2017. UV/chlorine as an advanced oxidation process for the degradation of benzalkonium chloride: Synergistic effect, transformation products and toxicity evaluation. Water Res 114, 246–253. https://doi.org/10.1016/j.watres.2017.02.015.

[26] Huh, D.S., Choe, S.J., 2010. Comparative DFT study for molecular geometries and spectra of methyl pheophorbides-a: test of M06-2X and two other functionals. J Porphyr Phthalocyanines 14 (7), 592–604. https://doi.org/10.1142/S1088424610002410.

[27] Hypercube, I., 2001. New Release 7 of HyperChem. October 15. Hypercube, Inc.,. October 15. ⟨http://www.hyper.com/?TableId=412⟩.

[28] Itoh, Y., Horiuchi, S., Yamamoto, K., 2005. Photo Surfactant: Photo 835–839.

[29] Jia, Y., Huang, Y., Ma, J., Zhang, S., Liu, J., Li, T., Song, L., 2024. Toxicity of the disinfectant benzalkonium chloride (C 14) towards cyanobacterium Microcystis

results from its impact on the photosynthetic apparatus and cell metabolism. J Environ Sci 135, 198–209. https://doi.org/10.1016/j.jes.2022.11.007.
[30] Joshi, D.K., Betancourt, F., Mcadorey, A., Yalagala, R.S., Poupon, A., Yan, H., 2023. Chemistry BODIPY quaternary ammonium salt as photosensitizers. J Photochem Photobiol, A: Chem 434 (August 2022), 114213. https://doi.org/10.1016/j.jphotochem.2022.114213.
[31] Krishnan, S., Rawindran, H., Sinnathambi, C.M., Lim, J.W., 2017. Comparison of various advanced oxidation processes used in remediation of industrial wastewater laden with recalcitrant pollutants. In: IOP Conference Series: Materials Science and Engineering, Vol. 206. IOP Publishing,, 012089.
[32] Koe, W.S., Lee, J.W., Chong, W.C., Pang, Y.L., Sim, L.C., 2020. An overview of photocatalytic degradation: photocatalysts, mechanisms, and development of photocatalytic membrane. Environ Sci Pollut Res 27, 2522–2565.
[33] Kuźmiński, K., Morawski, A.W., Janus, M., 2018. Adsorption and Photocatalytic Degradation of Anionic and Cationic Surfactants on Nitrogen-Modified TiO2. J Surfactants Deterg 21 (6), 909–921. https://doi.org/10.1002/jsde.12190.
[34] Lee, M.Y., Wang, W.L., Du, Y., Hu, H.Y., Huang, N., Xu, Z.Bin, Wu, Q.Y., Ye, B., 2020. Enhancement effect among a UV, persulfate, and copper (UV/PS/Cu2+) system on the degradation of nonoxidizing biocide: The kinetics, radical species, and degradation pathway. Chem Eng J 382 (March 2019). https://doi.org/10.1016/j.cej.2019.122312.
[35] Lee, M.Y., Wang, W.L., Wu, Q.Y., Huang, N., Xu, Z.Bin, Hu, H.Y., 2018. Degradation of dodecyl dimethyl benzyl ammonium chloride (DDBAC) as a non-oxidizing biocide in reverse osmosis system using UV/persulfate: Kinetics, degradation pathways, and toxicity evaluation. Chem Eng J 352 (April), 283–292. https://doi.org/10.1016/j.cej.2018.04.174.
[36] Lee, M.Y., Wang, W.L., Xu, Z.Bin, Ye, B., Wu, Q.Y., Hu, H.Y., 2019. The application of UV/PS oxidation for removal of a quaternary ammonium compound of dodecyl trimethyl ammonium chloride (DTAC): The kinetics and mechanism. Sci Total Environ 655, 1261–1269. https://doi.org/10.1016/j.scitotenv.2018.11.256.
[37] Li, D., Feng, Z., Zhou, B., Chen, H., Yuan, R., 2022. Impact of water matrices on oxidation effects and mechanisms of pharmaceuticals by ultraviolet-based advanced oxidation technologies: A review. Sci Total Environ 844, 157162.
[38] Li, X., Luo, X., Mai, B., Liu, J., Chen, L., Lin, S., 2014. Occurrence of quaternary ammonium compounds (QACs) and their application as a tracer for sewage derived pollution in urban estuarine sediments. Environ Pollut 185, 127–133. https://doi.org/10.1016/j.envpol.2013.10.028.
[39] Liu, C., Goh, S.G., You, L., Yuan, Q., Mohapatra, S., Gin, K.Y.H., Chen, B., 2023. Low concentration quaternary ammonium compounds promoted antibiotic resistance gene transfer via plasmid conjugation. Sci Total Environ 887, 163781. https://doi.org/10.1016/j.scitotenv.2023.163781.
[40] López Loveira, E., Fiol, P.S., Senn, A., Curutchet, G., Candal, R., Litter, M.I., 2012. TiO 2-photocatalytic treatment coupled with biological systems for the elimination of benzalkonium chloride in water. Sep Purif Technol 91, 108–116. https://doi.org/10.1016/j.seppur.2011.12.007.
[41] Lu, T., Chen, F., 2012. Multiwfn: A multifunctional wavefunction analyzer. J Comput Chem 33 (5), 580–592. https://doi.org/10.1002/JCC.22885.
[42] Lu, T., Chen, F., 2012. ATOMIC DIPOLE MOMENT CORRECTED HIRSHFELD POPULATION METHOD. J Theor Comput Chem 11 (1), 163–183. https://doi.org/10.1142/S0219633612500113.
[43] Mai, Y., Wang, Z., Zhou, Y., Wang, G., Chen, J., Lin, Y., Ji, P., Zhang, W., Jing, Q., Chen, L., Chen, Z., Lin, H., Jiang, L., Yuan, C., Xu, P., Huang, M., 2023, From disinfectants to antibiotics: Enhanced biosafety of quaternary ammonium compounds by chemical modification. https://doi.org/10.1016/j.jhazmat.2023.132454.
[44] Merino, F., Rubio, S., Pérez-Bendito, D., 2003. Mixed aggregate-based acid-induced cloud-point extraction and ion-trap liquid chromatography-mass spectrometry for the determination of cationic surfactants in sewage sludge. J Chromatogr A 998 (1–2), 143–154. https://doi.org/10.1016/S0021-9673(03)00565-X.
[45] Migueres, N., Debaille, C., Walusiak-Skorupa, J., Lipińska-Ojrzanowska, A., Munoz, X., van Kampen, V., Suojalehto, H., Suuronen, K., Seed, M., Lee, S., Rifflart, C., Godet, J., de Blay, F., Vandenplas, O., 2021. Occupational Asthma Caused by Quaternary Ammonium Compounds: A Multicenter Cohort Study. J Allergy Clin Immunol: Pract 9 (9), 3387–3395. https://doi.org/10.1016/j.jaip.2021.04.041.
[46] Miłosek, E., Kuźmicka, L., Karpińska, J., 2014. Direct and forced photodegradation of sodium dodecyl sulfate and tetraoctylammonium bromide. Toxicol Environ Chem 96 (1), 27–40. https://doi.org/10.1080/02772248.2014.909430.
[47] Mohapatra, S., Menon, N.G., Padhye, L.P., Tatiparti, S.S.V., Mukherji, S., 2021. Natural attenuation of pharmaceuticals in the aquatic environment and role of phototransformation. Contam Drink Wastewater Source: Chall Reigning Technol 65–94.
[48] Mohapatra, S., Mrozik, W., Acharya, K., Menon, N.G., 2022. Suspect and Nontarget Screening of Pharmaceuticals in Water and Wastewater Matrices. *Legacy and Emerging Contaminants in Water and Wastewater: Monitoring, Risk Assessment and Remediation Techniques*. Springer International Publishing,, Cham, pp. 77–92.
[49] Mohapatra, S., Yutao, L., Goh, S.G., Ng, C., Luhua, Y., Tran, N.H., Gin, K.Y.H., 2023. Quaternary ammonium compounds of emerging concern: Classification, occurrence, fate, toxicity and antimicrobial resistance. J Hazard Mater 445. https://doi.org/10.1016/j.jhazmat.2022.130393.
[50] Mohapatra, S., Bhatia, S., Senaratna, K.Y.K., Jong, M.C., Lim, C.M.B., Gangesh, G. R., Gin, K.Y.H., 2023. Wastewater surveillance of SARS-CoV-2 and chemical markers in campus dormitories in an evolving COVID− 19 pandemic. J Hazard Mater 446, 130690.
[51] Mohapatra, S., Snow, D., Shea, P., Gálvez-Rodríguez, A., Kumar, M., Padhye, L.P., Mukherji, S., 2023. Photodegradation of a mixture of five pharmaceuticals commonly found in wastewater: Experimental and computational analysis. Environ Res 216, 114659. https://doi.org/10.1016/J.ENVRES.2022.114659.
[52] Osimitz, T.G., Droege, W., 2022. Adverse Outcome Pathway for Antimicrobial Quaternary Ammonium Compounds. J Toxicol Environ Health - Part A: Curr Issues 85 (12), 494–510. https://doi.org/10.1080/15287394.2022.2037479.
[53] Panich, N.M., Seliverstov, A.F., Ershov, B.G., 2013. Photodecomposition of dodecyltrimethylammonium bromide in aqueous solutions in presence of hydrogen peroxide. Theor Found Chem Eng 47 (5), 629–632. https://doi.org/10.1134/S0040579513050072.
[54] Priyadarshini, M., Das, I., Ghangrekar, M.M., Blaney, L., 2022. Advanced oxidation processes: Performance, advantages, and scale-up of emerging technologies. J Environ Manag 316, 115295.
[55] Radke, M., Behrends, T., Förster, J., Herrmann, R., 1999. Analysis of cationic surfactants by microbore high-performance liquid chromatography-electrospray mass spectrometry. Anal Chem 71 (23), 5362–5366. https://doi.org/10.1021/AC990453Q.
[56] Rawat, J., Kandwal, P., Juyal, A., Sharma, H., Dwivedi, C., 2023. Synthesis and photocatalytic activity of polymer stabilized cadmium selenide quantum dots-titanium dioxide nanocomposites. Mater Today Proc 83, 48–52. https://doi.org/10.1016/j.matpr.2023.01.145.
[57] Serpone, N., 1996. Photo Surfactants Total Org Carbon Meas TiO2- Assist Photo Surfactants Hisao HIDAKA * Toshiya WATANABE * 45 (1).
[58] Stewart, J.J.P., 2013. Optimization of parameters for semiempirical methods VI: More modifications to the NDDO approximations and re-optimization of parameters. J Mol Model 19 (1), 1–32. https://doi.org/10.1007/S00894-012-1667-X/FIGURES/8.
[59] Stewart, J.J., 2016. Mopac2016. Stewart Comput Chem: Colo Springs, CO, USA *650*.
[60] Suchithra, P.S., Carleer, R., Ananthakumar, S., Yperman, J., 2015. A hybridization approach to efficient TiO2 photodegradation of aqueous benzalkonium chloride. J Hazard Mater 293, 122–130. https://doi.org/10.1016/j.jhazmat.2015.03.011.
[61] Thiel, W., 2005. Semiempirical quantum-chemical methods in computational chemistry. Theory Appl Comput Chem: First Forty Years 559–580. https://doi.org/10.1016/B978-044451719-7/50064-0.
[62] Tong, Y., Lu, P., Zhang, W., Liu, J., Wang, Y., Quan, L., Ding, A., 2023. The shock of benzalkonium chloride on aerobic granular sludge system and its microbiological mechanism. Sci Total Environ, 165010. https://doi.org/10.1016/j.scitotenv.2023.165010.
[63] Wacławek, S., Lutze, H.V., Grübel, K., Padil, V.V., Černík, M., Dionysiou, D.D., 2017. Chemistry of persulfates in water and wastewater treatment: A review. Chem Eng J 330, 44–62.
[64] Wan, H., Fang, F., Shi, K., Yi, Z., Lei, L., Li, S., Mills, R., Bhattacharyya, D., Xu, Z., 2023. pH-Swing membrane adsorption of perfluoroalkyl substances: Anion-exchange brushes and role of water chemistry. Sep Purif Technol 329, 1383–5866. https://doi.org/10.1016/j.seppur.2023.124800.
[65] Xiao, Z.Y., Huang, N., Wang, Q., Wang, W.L., Wu, Q.Y., Hu, H.Y., 2022. Advanced oxidation of dodecyl dimethyl benzyl ammonium chloride by VUV/UV/chlorine: Synergistic effect, radicals, and degradation pathway. Sep Purif Technol 292 (April), 121012. https://doi.org/10.1016/j.seppur.2022.121012.
[66] Yang, W., Cai, C., Wang, R., Dai, X., 2023. Insights into the impact of quaternary ammonium disinfectant on sewage sludge anaerobic digestion: Dose-response, performance variation, and potential mechanisms. J Hazard Mater 444, 130341. https://doi.org/10.1016/j.jhazmat.2022.130341.
[67] Yu, X., Kamali, M., Van Aken, P., Appels, L., Van der Bruggen, B., Dewil, R., 2021. Advanced oxidation of benzalkonium chloride in aqueous media under ozone and ozone/UV systems – Degradation kinetics and toxicity evaluation. Chem Eng J 413 (November 2020). https://doi.org/10.1016/j.cej.2020.127431.